International Journal of Disaster Risk Reduction 113 (2024) 104822

Contents lists available at ScienceDirect

International Journal of Disaster Risk Reduction

journal homepage: www.elsevier.com/locate/ijdrr

National risk assessment of Italian school buildings: The MARS project experience

Serena Cattari [a,*], Sara Alfano [a], Vincenzo Manfredi [b], Barbara Borzi [c], Marta Faravelli [c], Antonella Di Meo [c], Francesca da Porto [d], Elisa Saler [d], Andrea Dall'Asta [e], Laura Gioiella [e], Marco Di Ludovico [f], Ciro Del Vecchio [g], Carlo Del Gaudio [f], Gerardo Verderame [f], Natalino Gattesco [h], Ingrid Boem [h], Elena Speranza [i], Mauro Dolce [f], Sergio Lagomarsino [a], Angelo Masi [b]

[a] University of Genoa, Genoa, Italy
[b] University of Basilicata, Potenza, Italy
[c] European Centre for Training and Research in Earthquake Engineering (EUCENTRE), Pavia, Italy
[d] University of Padua, Padova, Italy
[e] University of Camerino, Camerino, Italy
[f] University of Naples Federico II, Naples, Italy
[g] University of Sannio, Benevento, Italy
[h] University of Trieste, Trieste, Italy
[i] Italian Civil Protection Department, Via Ulpiano 11, Rome, Italy

ARTICLE INFO

Keywords:
School buildings
Archetypes
Seismic maps
Fragility curve
Masonry
Reinforced concrete

ABSTRACT

Strategic buildings, such as schools, play a crucial role in civil society. They are essential not only for the well-being of communities but also for their significance during the emergency and recovery phases following an earthquake. Reliable risk assessment is a powerful tool for implementing effective mitigation strategies. While considerable work has been already done in the literature to develop fragility curves and risk studies for residential buildings, there remains a noticeable gap in addressing risk assessment for school portfolios. As part of the 2019–2021 MARS (Seismic Risk MAps) project, funded by the Italian Civil Protection Department and involving the ReLUIS consortium along with the EUCENTRE foundation, a specific task was dedicated to evaluating seismic risk for the Italian school buildings. In this context, eight research units combined their expertise to develop a consensus-based vulnerability model, known as the "School-MARS model". This model integrates fragility curves based on various approaches (i.e. empirical, mechanical-analytical, mechanical-numerical and hybrid) and is tailored to archetypes representative of the Italian school buildings. The main goal of the paper is outlining the methodology used to define the "School-MARS vulnerability model". Moreover, the paper demonstrates the application of the latter for performing intensity-based and time-based risk analyses. Specifically, the results are presented in terms of damage distribution and usability ratings expected for the entire stock of Italian school building. Notably, these results indicate that approximately 26 % of Reinforced Concrete (RC) buildings and 31 % of Unreinforced Masonry (URM) structures may become unusable due to potential earthquakes expected in the next 50 years.

* Corresponding author.
E-mail address: serena.cattari@unige.it (S. Cattari).

https://doi.org/10.1016/j.ijdrr.2024.104822
Received 4 April 2024; Received in revised form 11 September 2024; Accepted 12 September 2024
Available online 14 September 2024

1. Introduction

Schools play a central role in societies since education is not only one of the fundamental human rights, but is also a key driver of growth, competitiveness, and economic development [1]. In this context, the safety of schools against natural and man-made hazards is a prerequisite for learning activities [2], as explicitly recommended by the United Nations. In fact, the United Nations includes quality education in a safe environment among the 17 Sustainable Development Goals [3], and this principle is also stated by the World Bank, which declares that "school infrastructures meeting minimum standards for safety and inclusion are one of the four key actions to create the foundation for safe, welcoming, non-discriminatory learning environments" [1].

In contrast to this desired goal, data from the "Global Program for Safer Schools" [4] indicates that, major earthquakes over the past 50 years caused 99,000 deaths in schools worldwide and, looking ahead, global forecast estimates in the future about 2,500 fatalities and about $3 billion of direct losses per year.

These huge losses are primarily attributed to the significant seismic vulnerability of school buildings. Many of these structures were built with only gravity loads or with minimal lateral horizontal load considerations, often lacking specific anti-seismic criteria. This has been evident in past seismic events, such as those experienced in Italy [5].

Hence, a substantial effort is required to mitigate seismic risk for school infrastructure in earthquake-prone areas. This effort should encompass various and concurrent lines of actions including [6]: i) enhancement of knowledge; ii) reduction of vulnerability; iii) mitigation of the effects.

In Italy, following the 2002 S. Giuliano earthquake, an effort was made to implement a more comprehensive strategy for risk mitigation of public buildings. Specifically, OPCM 3274/2003 [7] mandated seismic vulnerability assessment for all strategic (e.g. hospitals) and critical buildings (e.g. schools). This included integrating modern criteria and the seismic classification introduced by the ordinance. Subsequently, significant retrofitting programs were funded in 2003 and in 2009, resulting in approximately 1350 strengthening interventions on strategic and critical buildings, a considerable percentage of which were for school buildings. Notably, the National Prevention Plan, coordinated by the Italian Civil Protection Department (ICPD) (Decree-Law 39/2009, converted into Law 77/2009), allocated around 1 billion euro in 2009, with additional funding since 2018. This plan financed retrofitting interventions for nearly 250 school buildings, representing 25 % of the total number of interventions [6].

Other Countries, such as Canada [8], Mexico [9], Japan [10], Turkey [11], Lebanon [12], El Salvador [13] and other multi-lateral agencies promoted retrofitting programs and supported actions aimed at improving the safety conditions of schools around the world, like as: Sendai Framework for Disaster Risk Reduction 2015–2030 [14]; Worldwide Initiative for Safe Schools [15]; the Global Alliance for Disaster Risk Reduction and Resilience in the Education Sector [16]; Learning in twenty-first-century schools [17]; UNESCO Guidelines for Assessing Learning Facilities in the Context of Disaster Risk Reduction and Climate Change Adaptation [18]; and International Finance Corporation [19], just to mention a few. Among these initiatives, the "Global Program for Safer Schools" [4], launched by the World Bank in 2014, seeks to stimulate large-scale investments aimed at enhancing the safety and resilience of school infrastructure vulnerable to natural hazards and improving the quality of learning environments for children. At present, the program has activities in over 20 countries covering about 500,000 schools and about $1.4 billion of investments [4].

To effectively address mitigation policies and prioritize large-scale actions, intervention programs require reliable risk assessment methodologies. Because school buildings exhibit specific features that distinguish them from ordinary structures (such as residential buildings), these methodologies must be properly developed to avoid possible inaccuracies in fragility and loss estimation [20]. Several studies in the literature aim to assess the safety condition of school buildings. They primarily refer to specific national portfolio of schools, such as those of Greece [21,22], Italy ([23–26]), Nepal ([27–30]), Iran ([31,32]), Pakistan [33], Mexico [34], Indonesia ([35–37]), Philippines [38]. In the context of the "Global Program for Safer Schools", the "Global Library of School Infrastructure" ([2,4]) aims at providing fragility and vulnerability functions for risk assessment and strengthening solutions for a wide collection of school building types around the world.

In Italy, specific research on the seismic risk of school buildings has been funded by local projects [39] as well as by the ICPD for several years. Among those funded by the ICPD, in 2018, the two centres of competence for seismic risk – i.e. the ReLUIS (Network of University Laboratories for Seismic Engineering) consortium and the EUCENTRE (European Centre for Training and Research in Earthquake Engineering) Foundation - supported the ICPD in developing national seismic risk maps for the residential building stock. This significant achievement was presented to EU, in accordance with EU decision 1313/2013. The current ambition is to extend the assessment to include additional crucial assets of the Country, with a prominent focus on school buildings.

In particular, the 2019–2021 MARS (Seismic Risk MAps) project [40], was funded by the ICPD within a specific agreement with the ReLUIS consortium along with the EUCENTRE foundation. The main goal of the MARS project (coordinated by Proff. S. Lagomarsino and A. Masi) was to update the national risk assessment released in 2018 (NRA 2018, [41]) and tackle the risk of further assets. A specific task, i.e. Task 4.7 (coordinated by Proff. S. Cattari and A. Masi), was devoted to the seismic risk assessment of school buildings at the national scale. In this framework, eight research units (RUs) – i.e. from the University of Genoa (UniGE-a coordinated by Prof. S. Lagomarsino and UniGE-b by Prof.S.Cattari), University of Basilicata (UniBAS by Prof. A. Masi), University of Padua (UniPD by Prof. F. da Porto), University of Camerino (UniCAM by Prof. A. Dall'Asta), University of Naples Federico II (UniNA by Prof. M. Di Ludovico), University of Trieste (UniTS by Prof. N. Gattesco) and EUCENTRE (by B. Borzi) – conveyed their approaches to define a consensus-based vulnerability model of the Italian school buildings. This vulnerability model, known as "School-MARS model", was then used to assess the seismic risk of Italian schools.

This paper outlines the methodological steps taken to establish the "School-MARS model" and, then, demonstrates the application of the latter for performing risk analyses on Italian school buildings. Section 1 provides the research topic background, while Section 2 presents an overview of the distinctive features of the Italian school buildings and introduces the taxonomy utilized in this risk analysis. In Section 3, the paper illustrates and compares the set of fragility curves as originally developed by the RUs involved in the task. Section 4 details the integration of these fragility curves to formulate the consensus-based “School-MARS model” and its validation process. Section 5 presents the results achieved so far regarding intensity-based and time-based seismic risk. These results were obtained by implementing such a vulnerability model on the IRMA platform which is capable of performing large-scale risk analyses. This Section also highlights the potential of the use of “School-MARS model” for future applications addressed to support the planning of mitigation actions. Finally, Section 6 discusses the ongoing development of the research and future challenges.

2. Italian school buildings

2.1. Overview of Italian code for school buildings

This section provides an overview of regulations that have influenced the design of school buildings over the years and, thereby, determined some of their distinctive factors.

The first and most important regulation was issued in 1975 [42]; that was specifically devoted to the school building design from the architectural and functional points of view. The latter introduced specific requirements for school buildings at each educational level, for example specifying the maximum number of storeys (i.e., one, two and three storeys for nursery, elementary/secondary and high schools, respectively). Considering its impact on exposure, it is worth noting that this regulation also established both the maximum number of classes per school (ranging from nine for nursery to sixty for high schools) and the maximum number of students per class (twenty-five). Additionally, it specified the reference surface per student, which ranges from approximately 7 m^2 for nursery to 12 m^2 for high schools.[1]

Further, the live load to be considered in structural design was set to 3.50 kN/m^2 (then reduced to 3.00 kN/m^2 in 1996 by Ref. [43]): a value higher than the one for ordinary (residential) buildings, which was equal to 2.0 kN/m^2 [44].

Considering the role of the seismic behaviour of both masonry and infill walls with openings [45], code requirements generally led to window dimensions of 1/5–1/7 for the net classroom surface, which is larger than the 1/8 reference value adopted for residential buildings [46].

From the structural point of view, aside from some variations in the intensity of live vertical and seismic loads, the design of schools has followed up to 2008 the same criteria of those used for other building types. It is worth mentioning that specific codes regulated the structural design of buildings subjected to gravity loads, with distinct requirements for the two most commonly used construction in Italy, i.e. unreinforced masonry (URM) and reinforced concrete (RC).

Regarding URM structures, no specific code existed until 1987, when the Ministerial Decree November 20, 1987 [47] introduced systematic prescriptions for guaranteeing the “box-like behaviour”, along with minimum reference values for mechanical properties and wall dimensions. Before this regulation, standard practices commonly led to quite flexible diaphragms and often lacked details to prevent out-of-plane failure mechanisms. Further, natural stone and clay bricks, commonly used in historical buildings built before 1920, were progressively replaced by hollow clay and concrete blocks.

Regarding RC buildings, the first regulation dated back 1939 when Royal Decree 2229/1939 [48] was issued. It provided some requirements in terms of minimum percentage of steel reinforcement and established some minimum values for materials mechanical properties. After the Law 1086 issued in 1971, which introduced significant prescriptions aimed to promote inspections procedures to certify the construction quality process, several Ministerial Decrees were issued recommending a better quality of materials along with some updating in terms of minimum requirements for structural members.

Regarding structural design in seismic areas, the first code [49] was issued after the 1909 Messina-Reggio Calabria earthquake, marking also the beginning of the seismic classification for the territory. It provided quite few specific requirements substantially related to URM buildings and introduced limitations in terms of height/number of storeys (e.g., no more than 2 storeys or 10 m in elevation, only one storey for “ordinary” masonry buildings). Subsequent introduced two different seismic categories [50], with horizontal loads set at 7 % or 10 % of the “seismic weight” for categories I and II, respectively [51]. However, these Codes did not include specific anti-seismic details, particularly for RC buildings.

The Ministerial Decree 19 June 1984 [52] was the first to prescribe an “importance coefficient” for schools and other critical buildings, increasing design seismic actions by 20 % compared to the standard ones applied to ordinary residential buildings.

A significant turning point came with the 2002 S. Giuliano earthquake, in the aftermath of which a new approach for the seismic classification was adopted and modern seismic principles were established in Codes. OPCM 3274/2003 [7] introduced major advancements in the design of new buildings and, especially, in the assessment of existing structures. These modifications were substantially aligned with Eurocode 8. Subsequently, Ministerial Decree January 14, 2008 [53] and Ministerial Decree January 17, 2018 [54] further updated the criteria introduced by OPCM 3274/2003, integrating all types of constructions to address both man-made and seismic hazards. According to these decrees, school buildings must be designed at least with a return period of 712 years, whereas for residential buildings the return period is 475 years. A discussion of the evolution of regulations in Italy and Europe, is provided in Ref. [55].

For clarity, Table 1 summarizes the key Italian Codes related to architectural, functional and structural requirements discussed above.

[1] These values include all school services such as gym, laboratories etc.

Table 1
Evolution of key codes issued in Italy that introduced regulations for school buildings covering architectural, functional and structural aspects.

Aspect	Structural Type	Decree number	Date	Main novelty introduced
Architectural/functional	All	Ministerial Decree December 18, 1975 [42]	1975	Design rules regulating, for example, the maximum number of storeys, the number of students per class and the reference surface per student. A reference live load value and window dimensions were introduced too.
Structural	All	Royal Decree n. 193, April 18, 1909 [49]	1909	First seismic classification and structural prescriptions in seismic areas.
	All	Royal Decree-Law March 13, 1927, n. 431 [50]	1927	Seismic classification according to two seismic categories (I and II), whose horizontal actions were set to 7 % and 10 % of the seismic weight, respectively.
	RC	Royal Decree 2229/1939 [48]	1939	First code providing requirements in terms of minimum percentage of steel reinforcement and allowable minimum mechanical properties of materials.
	RC	Law 1086/1971	1971	Relevant prescriptions for in-situ inspections for certifying the materials quality
	All	Ministerial Decree June 19, 1984 [52]	1984	Introduction of "importance coefficient" aimed to increase by 20 % the design seismic actions for school buildings compared to standards values adopted for residential structures
	Masonry	Ministerial Decree November 20, 1987 [47]	1987	First structural code for URM buildings that introduced minimum values for mechanical properties and wall dimensions, along with prescriptions to guarantee the "box-like behaviour"
	All	OPCM 3274/2003 [7]	2003	Introduction of principles of modern seismic engineering for design of buildings and updating of the seismic hazard classification
	All	Ministerial Decree January 17, 2018 [54]	2018	Last code in force that updated the design criteria introduced by OPCM 3274/2003, integrating all types of constructions to address both man-made and seismic hazards.

2.2. Available inventory and taxonomy adopted in the MARS project

The inventory of Italian school buildings available and used for 2019–2021 MARS research project was the one set up by the Ministry of Education in 2005, consisting of 49,531 assets. Although data for many schools, particularly those from specific regions, are incomplete or not available (see Figs. 1 and 2), this inventory provided valuable information for performing a seismic risk assessment. The inventory includes not only typological data (i.e. structural material, period of construction, number of storeys, plan area, type of vertical/horizontal/roof structures) but also administrative details (e.g., school name, address, and level of education). Moreover, it is worth highlighting that data is primarily collected by non-technician personnel, such as school principals or administrative officers.

Based on these data, which were adequately integrated and/or validated with local information provided by the RUs involved in the MARS project, some attributes primarily affecting the seismic vulnerability of existing buildings have been selected and considered for addressing the goals of this study. Specifically, they consist of:

- Structural material (i.e., reinforced concrete (RC), masonry (URM), Other);
- Number of storeys (i.e., 1, 2, 3, 4+);

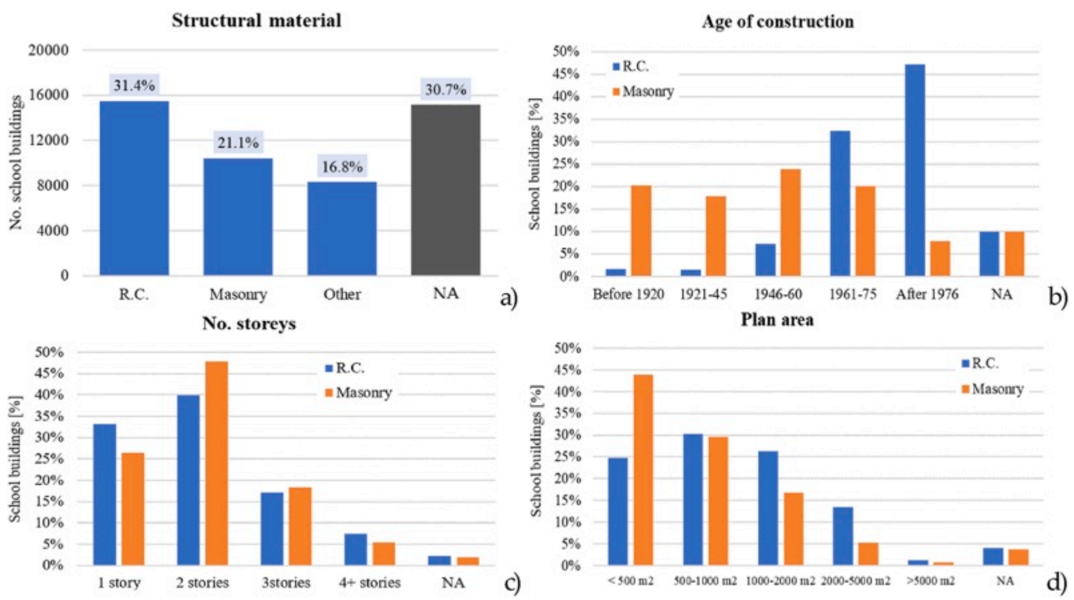

Fig. 1. Inventory of Italian school buildings in terms of structural material (a), construction age (b), number of storeys (c), and plan area (d) (adapted from Ref. [56]). Note that "NA" stands for "Not Available".

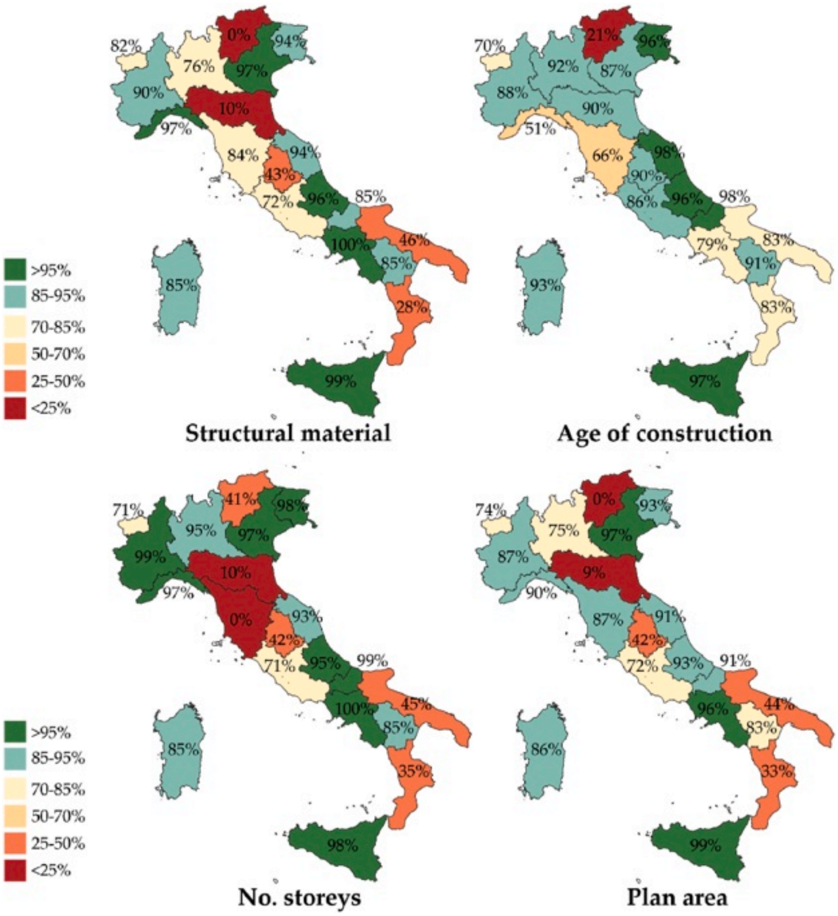

Fig. 2. Percentages of available data for the parameters selected from the taxonomy to describe the seismic vulnerability of school buildings (i.e. structural material, age of construction, number of storeys and plan area). The percentages are specified for each Italian region. The colours in the legend clarify the data completeness. (For interpretation of the references to colour in this figure legend, the reader is referred to the Web version of this article.)

- Age of construction (i.e., before 1920, 1921–45, 1946–60, 1961–75, after 1976);
- Plan area (<500 m^2, 500–1,000 m^2, 1,000–2,000 m^2, 2,000–5,000 m^2, and $>5,000$ m^2).

Note that the "Other" category encompasses buildings made up with various structural materials, such as steel or precast concrete. Similarly, "NA" (i.e. not available) denotes that information regarding the structural material or construction date is currently missing. The following vulnerability analyses and risk assessments pertain exclusively to RC and URM school buildings.

The list of such attributes defines the simplified taxonomy adopted in the MARS project for school buildings. The apparently short list of attributes reflects the need to focus on factors well-recognized in discriminating the seismic behaviour while ensuring that the data are available along the whole country for guaranteeing the proper association to fragility curves. Furthermore, this selection includes parameters that are already recognized as fundamental in seismic studies specifically related to school buildings, such are those introduced by the GLOSI taxonomy illustrated in Ref. [2]. Specifically, within GLOSI taxonomy, the primary factors include the main structural system, the height range and the seismic design level while the plan area falls into the secondary category. Regarding the seismic design level, it is noteworthy to highlight that the age of construction can be regarded as a proxy for it, as it is closely correlated with the evolution of Codes/Standards (see Section 2.1) and, consequently, the structural details adopted for the design.

According to the adopted taxonomy, most of the school buildings consist of RC structures (approximately 31 % with moment-resisting frames) and URM structures (about 21 % with regular or irregular masonry types). RC structures were mainly constructed starting from the 1960s, while the URM buildings predominantly date from before the 1960s. Both RC and URM school buildings generally have 1-2 storeys in elevation. For URM school buildings, approximately 45 % have a plan area of less than 500 m^2. In contrast, RC school buildings exhibit a more balanced distribution across area categories, with about 25–30 % each in the <500 m^2, 500–1,000 m^2 and 1,000–2,000 m^2 ranges.

The inventory considered does not differentiate each structural unit based on their usage (e.g., classrooms, auditoriums, gyms, etc.). Therefore, although it is worth noting that buildings used for common areas such as auditoriums and gyms typically have structural schemes characterized by large spans and are often constructed with precast concrete or steel, these distinctions could not be made in the inventory. Furthermore, since materials other than reinforced concrete and masonry are categorized as "Other", which is not included in this study, the fragility curves and risk analyses presented should be interpreted as specifically referring to classroom buildings.

Fig. 2 illustrates the completeness of data available for the four attributes considered in the taxonomy. The legend used is consistent across all attributes, enabling for a qualitative comparison of the available information across various regions. The figure highlights that, in some regions, data completeness is lacking for most of the parameters. This information is crucial for guiding future targeted actions and assessing areas where risk assessments might be affected by higher level of uncertainty, often due to difficulties in accurately attributing features to the school building stock.

3. Methodology adopted for deriving the set of fragility curves

3.1. Background and overview of the adopted approaches

Each RU involved in the MARS-Schools project studied and investigated the specific behaviour of the Italian school buildings using different computational models to derive fragility curves. These adopt a lognormal format and are associated with five damage levels (DLs) conceived to be compatible with the European Macroseismic Scale EMS-98 [57].

Among those available in the literature (e.g. Ref. [58]), the approaches adopted by RUs can be grouped into four macro-approaches, namely:

- *Empirical approach*, based on the use of observational data. In this case, two main approaches were adopted: the pure empirical approach, based on the direct fitting of observed data (by UniNA and UniCAM); and an empirical-binomial approach that exploits the simulated damage probability matrix using the binomial probability density function, ensuring a more regular distribution of damage states (by UniNA);
- *Mechanical-numerical approach*, based on Nonlinear Dynamic Analyses (NLDA) on detailed models inspired by the reference archetypes described in Section 3.2 (by UniBAS, UniCAM, UniNA, UniPD). At this stage of the research, this approach has been adopted only for RC school buildings;
- *Mechanical-analytical approach*, based on simulating the structural response through the use of simplified models that require a limited number of geometric and mechanical parameters and corrective factors to account for structural details (by UniGE-b and UniTS);
- *Hybrid approach*, that combines at least two of the aforementioned approaches. More specifically: i) the heuristic approach adopted by UniGE-a that aims at guaranteeing a fairly well fitting with actual damage but, at the same time, ensuring physically consistent results for increasing values of seismic intensity, thanks to the expertise that is implicit in the EMS-98 [57]; ii) the hybrid mechanical-analytical approaches adopted by UniNA and EUCENTRE, which make use also of some factors calibrated through observed damage evidence; iii) the hybrid method adopted by UniPD based on the integrated use of mechanical-analytical and macroseismic approaches [59].

Most of these methods were already developed and extensively validated [60] within the context of the Italian National Risk Assessment (NRA 2018) promoted by the ICDP [41], with specific reference at that time to the residential building stock, and adapted in this study to school buildings characteristics. A brief description of the different approaches used by each RU within the MARS-Schools project, along with their intrinsic pros and cons, is provided in the following section while interested readers are invited to deepen the respective references for a more detailed description of each method.

3.1.1. Empirical approaches

The *pure empirical approach* adopted by UniNA RU makes use of a (lognormal) statistical model directly fitted to observational data. This approach is similar to the one used in the NRA 2018 framework for residential buildings ([61,62]). The parameters of these fragility curves are estimated by maximizing the likelihood function through an optimization algorithm. The algorithm assumes that the counts of buildings experiencing a given damage grade in a specific Peak Ground Acceleration (PGA) bin follow a multinomial distribution. During the optimization procedure, the whole set of five fragility curves for a specific building class is simultaneously fitted to the observational data. This is done by assuming a common value for the logarithmic standard deviation for all the fragility curves, while allowing different values for the logarithmic mean. Instead, the *empirical-binomial approach* by UniNA is used to address the issue of irregularity and scarcity of damage data by assuming a continuous trend based on real observations. Previous studies have demonstrated that a binomial probability density function ([59,63,64]) or a beta probability density function [65] can effectively reproduce the observed damage frequencies. To account for this, the counts of buildings experiencing a specific damage grade within a particular PGA bin are “adjusted” using the binomial distribution as a function of the observational mean damage value. The same optimization procedure adopted for the pure empirical approach is then applied to the “adjusted” counts of damaged buildings to determine the unknown parameters of lognormal fragility curves. This approach helps mitigate the limitations of irregular and sparse data by capturing the underlying continuous trend derived from observational data. Further details on these two approaches - when specifically applied to the school buildings hit by the 2009 L'Aquila earthquake - are illustrated in Ref. [66].

The fragility curves presented by the UniCAM RU are directly derived from an *empirical predictive model* of damage ([67,68]), based on the analysis of data coming from post-earthquake surveys of the schools located in the nearby epicentres of the mainshocks of the 2016 Central Italy seismic sequence. The proposed probabilistic model provides a continuous description of the consequences in terms of intensity-based damage index. The parameters of the model are determined by inference techniques. The efficiency of the model relies on properly defined shape functions, able to describe the variability of the response by varying the intensity of the seismic action. This probabilistic response model can be also used to derive traditional fragility functions referred to as discrete classification of damage based on a proper selection of the response thresholds [57], while two different proposals for the classification of the DLs have been assumed according to the studies of [69,70].

Since the above-described methods use damage data from post-earthquake surveys to derive fragility functions, they intrinsically account for the variability of both building types and earthquake characteristics of the considered area. However, the reliability of these fragility functions is strongly affected by the quality and completeness of the database, as well as the capability of a set of buildings belonging to one, or more than one, specific areas to be representative of buildings of an entire country. Moreover, regarding the seismic input, it is worth noting that the empirical fragility curves here presented have been derived using traditional shakemaps, which start with the definition of a grid and a calculation based on Ground Motion Prediction Equations (GMPEs), conditioned on the real measurements (i.e. INGV broadband and the Italian Strong Motion Network - Rete Accelerometrica Nazionale). Such an approach is affected by the uncertainty deriving from that of GMPE used to characterize it. It is worth mentioning that some studies available in the literature highlighted the role of spatial and inter-period correlation in the intra-event ground motion residuals [71] as well as that of damage data in informing better the input at the site [72], both aspects that could be further investigated in future developments.

3.1.2. Mechanical-analytical approaches

The *mechanical-analytical approach* adopted by UniGE-b RU consists of the DBV-Masonry model, where DBV stands for Displacement Based Vulnerability. The model is based on the proposal previously described in ([73,74]), and further updated within the MARS project by Ref. [75]. According to Ref. [74], the structural response is described in terms of a capacity curve which requires defining a limited set of mechanical and geometric parameters, assuming a fundamental modal shape, and applying specific correction factors to account for the effects related to structural and morphological details typical of existing buildings (e.g., presence or absence of steel tie-rods or RC ring beams). The analytical derivation of the main parameters that define the capacity curve (namely the initial period, the acceleration at yielding, and the displacement capacity associated with four damage levels explicitly computed) makes primary reference to the activation of the in-plane response of URM walls, under the assumption of a "box-like behaviour". The displacement capacity moreover analytically considers the activation of possible in-plane mechanisms, such as "uniform" (with a damage primarily concentrated in spandrel) or "soft-story" (with damage primarily concentrated in pier located at ground floor), and explicitly also thredols values of URM piers. Then, within the MARS project, additional corrective factors have been introduced to account also for the possible activation of local mechanisms associated with the out-of-plane response. The latter parameters are assumed to possibly reduce the displacement capacity assessed for the full exploitation of the global response. For the definition of fragility curves, a nonlinear static procedure - based on the use of the Capacity Spectrum Method (CSM) and overdamped spectra [76] - is adopted to compute the value of the intensity measure that triggers each DL [57], while the response surface technique (RST) is used for propagating capacity uncertainties and finally deriving the fragility curves [73]. The method allows to consider both the intra-building variability through the RST and the inter-building variability depending on the number of analyzed archetypes.

Regarding the *mechanical-analytical* methodology defined by UniTS RU, simplified lateral load-displacement capacity curves were drawn for real school buildings by using the "Firstep-M" algorithm [77]. The tool allows an estimation of the building's lateral stiffness and resistance (in the two main directions) by evaluating the elastic distribution of a unitary force among the vertical panels (i.e. piers) at the ground floor. In the case of rigid diaphragms, the redistribution of the shear force among piers is also assumed. Both shear and bending failure in the piers are considered. The ultimate drift is based on the dominant failure mode, according to the values provided in the literature. Similarly to DBV-Masonry model, the maximum accelerations compatible with the attainment of various damage levels were then calculated by applying the CSM and adopting overdamped spectra [76]. However, these values are "deterministic" for each examined archetype. Then, the source of uncertainty explicitly computed by this method for deriving fragility curves is only associated to inter-building variability and depends on the number of analyzed archetypes.

The adopted mechanical-analytical methods, as well as the other ones available in the literature, are based on models that incorporate simplified assumptions to reduce the computational burden compared to refined 3D model. These models operate within a displacement-based framework, allowing for the description of the seismic input using the acceleration-displacement response format. This feature makes them more versatile. Moreover, they can be easily applied to a large number of building archetypes by explicitly considering key attributes of the building stock under examination, as well as various sources of uncertainties. This approach therefore enables the simulation of the seismic response of different building types, including high-intensity seismic input values, for which not enough robust empirical data are generally available.

However, the main limitations include the simplifications inevitably introduced by structural modelling, which reduce the models' capability to account for the full complexity of existing buildings. These simplifications are in fact often addressed through corrective factors. Additionally, the assessment of estimate of PGA associated with the attainment of DLs relies on nonlinear static procedures, which are a simplification of more accurate NLDAs. Consequently, while these methods can potentially account for the intra- and inter-buildings variability, they are less precise in estimating seismic input uncertainty.

3.1.3. Hybrid approaches

In this study different kinds of *hybrid approaches* have been considered.

The *heuristic model* developed by UniGE-a starts from the original proposal of the macroseismic method illustrated in Ref. [59] and, recently, further refined thanks to the availability of damage data collected after many Italian earthquakes. Specifically, the refinement for residential buildings was completed in Ref. [64] using the data collected in D. a.D.O platform (Observed Damage Database) [78], while, for the Italian school buildings, it was based on the data collected following the 2009 L'Aquila earthquake, as detailed in Ref. [66]. The method is based on the expertise that is implicit in the EMS-98 scale [57], which assumes a regular increase of the mean damage (μ_D) with the earthquake intensity (I). In particular, in Ref. [59] the vulnerability curves were originally derived with fuzzy assumptions on the binomial damage, establishing an analytical correlation between μ_D and I through the introduction of two parameters, namely the vulnerability index (V) and the ductility index (Q). In Refs. [64,66], the V and Q parameters have been derived based on the fitting of the vulnerability curve through the available real observed data. Then, the introduction of a correlation law between PGA and I and the assumption of the binomial distribution allow passing to the fragility curves.

As for the *hybrid mechanical-analytical* approaches, they are proposed by UniNA, with the POST (PushOver on Shear Type models) model [79,80], and EUCENTRE with the SP-BELA (Simplified Pushover-Based Earthquake Loss Assessment) model [81]. Both methods refer only to RC structures.

In the POST method adopted by UniNA, according to Ref. [82], the building's structural model is generated using a simulated design process in accordance with the design code requirements, professional guidelines, and seismic classification relevant to the specific location during the construction phase. Subsequently, the building response is evaluated using a 3D frame model which assumes a shear-type behaviour. Thanks to this hypothesis, the nonlinear shear-displacement behaviours of all RC columns and infill panels can be assumed to act in parallel at each storey. By considering these shear-displacement response curves at each storey, along with a predetermined lateral force distribution, the pushover curve is analytically obtained in closed form. The evaluation of seismic capacity in terms of spectral intensity is performed within the SPO2IDA framework [83]. This assessment is carried out at specific performance levels (PLs), which are determined by establishing a correspondence between PLs and the damage classification suggested by EMS-98 [57]; in defining the DLs, the procedure introduces also some calibration of inter storey drift thresholds based on evidence from real observed data (i.e. that is the aspect that justifies the classification of the method as hybrid). Finally, a Monte Carlo simulation technique is used to repeatedly apply the above procedure. Random variables are introduced to account for the inherent uncertainty in the geometrical/mechanical parameters, and in models/response parameters. This ensures propagating the aleatoric and epistemic uncertainties in the final outcomes, obtaining a distribution of PGA capacity. Its cumulative frequency distributions, herein adopted to represent fragility curves for the considered building class and the adopted damage classification, provide information on the exceeding probability of damage.

EUCENTRE, instead, proposes fragility curves calculated using the SP-BELA methodology, already adopted for residential buildings [84] but adapted in this study to be representative of the geometry and characteristics of school buildings. SP-BELA starts from a prototype building that represents the considered typology, and creates with Monte Carlo generation a sample of buildings, each one then subjected to a nonlinear static analysis that allows its pushover curve to be evaluated. Finally, by comparing the capacity of each building with the demand in a displacement-based framework, the probability of exceeding damage levels is computed. The curves obtained were calibrated by comparing the numerically calculated damage scenarios with the observed damage data from the Da.D.O. platform [78]. In the aforementioned comparison, both structural and non-structural damage have been considered, dominating severe/heavy and collapse damage levels and lower damage levels, respectively.

The *hybrid mechanical-macroseismic approach* adopted by UNIPD is based on the simplified mechanical approach Vulnus ([85–87]), which analyses masonry buildings by evaluating both their in-plane base shear capacity and the triggering of out-of-plane mechanisms, as well as a series of qualitative vulnerability factors which derive from the II level GNDT form for URM buildings ([88,89]). Fuzzy logic is then applied to derive fragility sets for a specific damage state. These sets are then extended to the five DLS from EMS-98 [57] by adopting as reference for the spacing among fragility curves the macroseismic model proposed in Ref. [59].

According to the definition used in the literature, the considered hybrid approaches are based on a combination of both analytical and observational data, also completed by expert judgment. The main advantage is that they can integrate the scarcity of observational data by using analytical results and vice-versa. Additionally, empirical data from post-seismic observations are used to calibrate some parameters in the procedure of fragility curve derivation. However, these approaches incorporate the main limitations of the individual methods they combine, as detailed in Sections 3.1.1 and 3.1.2.

3.1.4. Mechanical-numerical approaches

The *mechanical-numerical approaches* make use of NLDA on detailed models for deriving fragility curves. So far this approach has been used in MARS project only for RC school buildings. Details on the modelling strategy adopted by each RU are provided in the following. Instead, for what pertains the other common assumptions adopted for postprocessing the results of NLDA (e.g. selection of records, selection of the Engineering Demand Parameter), a more in-depth discussion is carried out in Section 3.3. In all cases, numerical models reproduce some of the archetypes illustrated in Section 3.2.

UniBAS RU modelled each structure in the framework of the Opensees platform [90] by following the same lumped plasticity strategy reported in Ref. [91] for residential building types.

Three-dimensional Finite Element Models (FEMs) have been instead developed with the SAP2000 software [92] by UniCAM RU. The models account for the hysteretic behaviour of the structural members through plastic hinges located at the ends of beams and columns.

Also, for UniNA RU, the nonlinear numerical model was built in the SAP2000 software [92] environment, considering a lumped plasticity approach. The plastic hinges were characterized considering cracking, yielding, ultimate rotation according to the Eurocode 8 (2005). Post peak degradation was characterized according to Ref. [93] and a pivot model was used to reproduce the cyclic response [94], calibrating the parameters to match the hysteretic response and energy dissipation of RC members typical of the Italian construction standards [95]. More details on the modelling approach can be found in Ref. [96].

Finally, the UniPD RU simulated an archetype – that was designed only for gravity loads - through a fiber model [97] and using the software Midas GEN [98]. Differently from the other models set by the other RUs, masonry infills are explicitly considered in the model, through a single-strut macro-model ([99,100]) with lumped plasticity, defined according to the constitutive law proposed by Panagiotakos and Fardis [101].

Similar to analytical-numerical approaches (see Section 3.1.2), mechanical-numerical methods simulate the seismic response using models selected to be capable for including the key attributes of a given building stock. However, to overcome some intrinsic limitations of mechanical-analytical methods, the considered mechanical-numerical methods employ more refined modelling of structural and non-structural components, along with more accurate analyses methods based on non-linear time history analyses using a properly defined set of signals As a result, these methods effectively account for record-to-record variability. However, due to the significant computational effort required, only a limited number of archetypes are generally analyzed: a limitation which can affect the estimation of some sources of uncertainty, such as inter-building variability. Additionally, in the MARS project, so far, mechanical properties of these numerical models are assumed deterministic, therefore also the uncertainty associated to the capacity is not explicitly estimated.

3.2. Definition of reference archetypes

Based on the taxonomy introduced in Section 2.2, the sub-types used for developing fragility curves are derived from a combination of the considered attributes, i.e., structural type, plan area, number of stories, and period of construction (as detailed in Table 2).

To define the reference archetypes representing the Italian school building stock, the most populated sub-types - i.e. those covering a large percentage of the school building stock - were selected. Specifically, five sub-types have been defined for each structural material, as detailed in Table 2. These sub-types account for 79 % of URM buildings and 85 % of RC ones, respectively. Fig. 3, by way of example in the case of URM school buildings, clarifies the criteria adopted for such a selection. The first three figures show the cumulative distribution by construction age, number of storeys and plan area, while the fourth figure highlights that URM schools with two storeys and area lower than 500 m^2, built before 1919 (sub-type 3), and those with one or two storeys built between 1920 and 1975 (sub-types 1 and 2) are among the most common (covering the 35 % of the total stock). A similar analysis was conducted for RC school buildings to identify the five sub-types summarized in Table 2.

For each sub-type, archetypes have been selected based on the completeness and reliability of the available data. Specifically, at the current state of the research, a total of 14 URM and 18 RC archetypes were chosen. These prototype buildings were selected by the various RUs using databases from previous detailed studies. The selection focused on structures with sufficiently complete data to be modelled using both simplified mechanical-analytical models and detailed numerical models adopted for the NLDA. The Annex I provides the in-plan view of the URM and RC archetypes, respectively.

These archetypes were used either in their “as is” (i.e., original) configuration or in a “propagated” configuration to represent other sub-types (e.g., belonging to different construction ages). The “propagated” configuration means that, while the geometrical data (both in-plan and in-elevation) were maintained, structural details (such as presence of tie-rods or RC beams), material properties (including the wall's thickness) and diaphragms types (e.g., timber, RC, or vaults) were varied.

3.3. Overview of the common hypotheses shared among RUs

Despite the intrinsic differences in all the approaches illustrated in Section 3.1 – which, at the same time, represent one of the project's most valuable resources-the RUs have, whenever possible, shared common basic assumptions to ensure an appropriate comparison of results.

First of all, as already mentioned, each RU developed fragility curves to be conceptually consistent with the five damage levels (DL_i, i = 1 … 5) defined in the EMS-98 [57]. Fragility curves refer to the lognormal cumulative distribution format, which, as well known, requires the definition of two main parameters: the median value of the lognormal distribution of the intensity measure (in this case the PGA_{DLi}) for which the DL is attained; and its dispersion.

In the following, additional clarifications are provided on the building stock used as a reference to for deriving the fragility curves.

The heuristic and empirical methods by UniGE and UniNA RUs refer to the URM and RC school buildings of the Abruzzo region hit by the L'Aquila 2009 earthquake, while the empirical approach of UniCAM RU refers to the school buildings stock of the Marche region damaged by the 2016/2017 Central Italy earthquake. A more detailed description of such samples is provided in Refs. [10,18], respectively.

Table 2
Sub-types and relative percentage for masonry and reinforced concrete school types.

n. subtype	Masonry		RC	
	description	**% of total schools**	**description**	**% of total schools**
1	area < 500 m^2 n. storey = 1 period: 1920–1975	13.6	area < 500 m^2; n. storey = 1 period: All	13.3
2	area < 500 m^2; n. storey 2 and 3; period: 1920–1975	19.5	area < 500 m^2; n. storey 2 and 3; period: All	10.9
3	area < 500 m^2; n. storey = 1, 2 and 3; period: before 1919	7.9	area = 500–1,000 m^2; n. storey = 1, 2 and 3; period: All	29.8
4	area = 500–1,000 m^2; n. storey = 1, 2 and 3; period: after 1975	27.0	area = 1,000–2,000 m^2; n. storey = 2 and 3; period: All	19.5
5	area = 1,000–2,000 m^2; n. storey = 1, 2 and 3; period: after 1975	10.5	area = 2,000–5,000 m^2; n. storey = 2 and 3; period: All	11.4

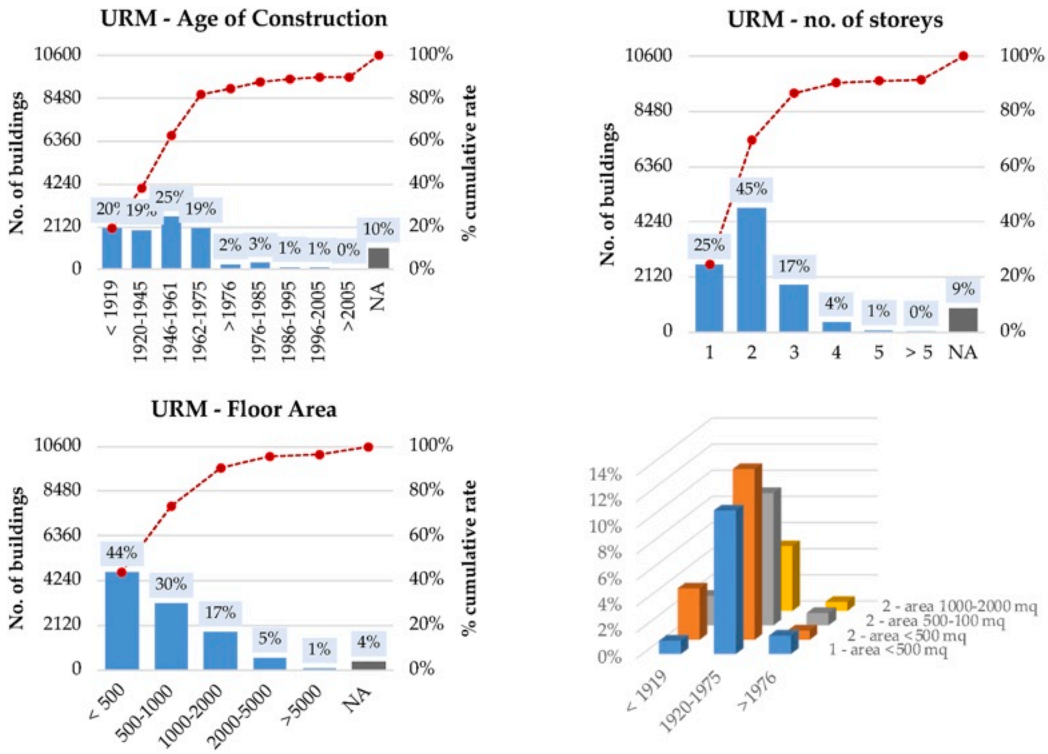

Fig. 3. Cumulative distributions that justify the selection of most populated sub-types – and consequently addressed the archetype choice - in the case of URM school buildings.

For URM school buildings, both the mechanical-analytical model developed by UniGE and the hybrid model adopted by UniPD utilized the archetypes illustrated in Section 3.2. Additionally, the two RUs employed a consistent procedure to extend the "as is" configuration of the archetypes to parametric configurations that represent an entire sub-type (i.e. generalize and "propagate" them). This procedure includes rules for adjusting wall thickness based on the masonry type (to ensure plausibility and adherence to rules of the art), modifying load distributions across diaphragms based on their structural typology (whether timber, RC or vaults), and adapting mechanical parameters according to masonry type or to account for different structural details. The approach adopted for such a generalization is illustrated in Ref. [75].

Conversely, the analytical-mechanical model developed by UniTS refers to a database including about 100 school buildings located in Friuli-Venezia Giulia (FVG) region. All these buildings have been analyzed in their "as is" configuration and grouped according to the taxonomy described in Section 2 for estimating the inter-building variability.

Table 3 summarizes for URM school buildings: the approach adopted by the RU; the name of the model adopted by the RU; the reference building stock used for developing fragility curves (see also Section 3.2); and, the main references which interested readers may invited referring for a more in-depth examination of key concepts of each method.

With the exception of UniTS and UniCAM, all other RUs provided fragility curves for the complete set of identified sub-types and potentially ready to be applied to schools with fully populated database fields. UniTS did not provide results for certain sub-types – representing approximately 950 schools across Italy – due to insufficient data coverage in the adopted FVG database. In contrast, UniCAM developed a single global curve representing all URM schools. Additionally, this single fragility curve is not differentiated by the

Table 3
Approaches adopted by each research unit to define fragility curves for URM school buildings.

Approach	Research unit & Approach name	Reference school buildings stock	Analyzed archetypes	References
Empirical and empirical-binomial	UniNA	School buildings of the Abruzzo region hit by the L'Aquila 2009 earthquake	–	[66]
Heuristic	UniGE-a			
Empirical	UniCAM	School buildings hit by the 2016–2017 Central Italy earthquake	–	[67]
Mechanical-analytical	UniGE-b (DBV-Masonry)	Archetypes defined in MARS project - Task 4.7	All	[75]
	UniTS (Firstep-M)	School buildings of Friuli-Venezia Giulia region	–	[102]
Hybrid mechanical-analytical/macroseismic	UniPD (VULNUS)	Archetypes defined in MARS project - Task 4.7	All	[103]

number of storeys or construction age because the available data were not statistically robust enough to support a direct empirical fitting of sub-types.

For RC school buildings, the mechanical-analytical models developed by EUCENTRE and UniNA utilized as starting reference the archetypes illustrated in Section 3.2. Both RUs adopted some similar simplifications in their planimetric configurations due to some limitations in capturing strong irregularity in the structural scheme. These approaches have provided fragility curves for all sub-types of RC schools. For the mechanical-numerical approach based on NLDAs, building response has been simulated by taking into account most of the failure mechanisms which may potentially affect both structural and non-structural components. At the current state of the research, this approach has been applied to two structural configurations, one designed only for vertical gravity loads and another one designed for low horizontal seismic forces. A total of 7 archetype buildings have been analyzed (see Section 3.2), specifically inspired by archetypes no.3/5/7/13/15 of Figs. I and II reported in Annex I. Table 4 summarizes for RC schools the same information presented in Table 3 for URM schools.

Regarding the NLDAs, which have been performed only for RC school buildings, each RU adopted a different modelling software based on their specific expertise (as described in Section 3.1). However, all RUs adopted common assumptions for conducting and post-processing the analyses to minimize uncertainties when comparing the results.

NLDAs were performed with a Cloud-like method [107], using a large dataset of signals [108] consisting of 125 real accelerograms with no or limited scaling factors. The signals have been selected to match the Italian code-conforming spectra defined with increasing intensity (i.e. return periods going from 50 to 10,000 years), for subsoil rock category A and B [54]. Cloud NLDAs have been performed considering 250 time-histories per building (125 couples of accelerograms with components applied alternatively along the two horizontal directions). The methodology involves performing NLDAs for increasing intensities of seismic excitation to explore increasing structural damage states. The results were interpreted with a centralized procedure by establishing a correlation between a parameter representative of the seismic response (Intensity Measure - IM) and the overall damage level simulated by the numerical model (Engineering Demand parameter - EDP). Regarding the IM, the PGA has been chosen as the best compromise between a good correlation with the non-linear response and practical constraints (e.g. characteristics of the IRMA platform used for risk analyses and illustrated in Section 5). For each analysis, the maximum inter-story drift value (IDR, assumed as EDP) between the two in-plane directions has been collected and then processed by considering the EDP-damage levels relationship reported in Ref. [90]. The IDR values falling within the specific ranges adopted for each five damage levels were collected, and the corresponding PGA values were then used to derive fragility curves, assuming a lognormal distribution function. The IDR thresholds defined for reaching each DL (shown in Table 5) were shared among the RUs with the aim of ensuring conceptual consistency with the EMS-98 [57]. The values have been established starting from previous studies related to residential buildings and properly modified to account for the specific characteristics of school buildings (e.g. large openings). Additionally, note that the school buildings analyzed through NLDAs have the same infill type, which predominantly influences the damage levels up to DL3, and poor seismic details, which affect mostly the higher damage levels. These similar features of archetypes justify the adoption of a single set of reference thresholds.

Several preliminary sensitivity analyses were carried out for the definition of the PGA value to be used as a reference. Specifically, the following alternatives were explored: the maximum PGA between the two directions (PGA_{max}); the geometric mean between the PGA of the two directions (PGA_{mean}); the PGA value corresponding to the component that causes the maximum inter-storey drift between the two in-plane horizontal directions (PGA_{rel}). This latter value has been determined also considering the effect of applying

Table 4
Approaches adopted by each research unit to define fragility curves for reinforced concrete schools.

Approach	Approach's name or Software adopted & RU	Reference school buildings stock	Analyzed archetypes	References
Empirical and empirical-binomial	UniNA	School buildings of the Abruzzo region hit by the L'Aquila 2009 earthquake	–	[66]
Hybrid Heuristic	UniGE-a			
Empirical	UniCAM	School buildings hit by the 2016–2017 Central Italy earthquake	–	[67]
Hybrid -mechanical-analytical	UniNA (POST)	Archetypes defined in MARS project (Task 4.7)	13 (2 SU)	[104]
	EUCENTRE (SP-BELA)		3-9-13 (4 SU) −15	[84]
Mechanical-numerical	UniNA (SAP 2000)	Archetypes defined in MARS project (Task 4.7) (for a total of 7 schools)	5	[105,106]
	UniBAS (OpenSees)		3	
	UniPD (MIDAS)		7–15	
	UniCAM (SAP 2000)		13 (3 SU)-5	

Table 5
IDR thresholds adopted for the achievement of each DL in the post-processing of cloud-NLDAs.

Damage level (DL)	IDR [%]
DL1	$0.1 \leq IDR < 0.25$
DL2	$0.25 \leq IDR < 0.5$
DL3	$0.5 \leq IDR < 1$
DL4	$1 \leq IDR < 2.5$
DL5	$IDR \geq 2.5$

the set of signals alternately along the two horizontal orthogonal directions. The analyses carried out showed that PGA_{max} is always the most optimistic, while the evaluations carried out with PGA_{mean} are those that lead to more punitive results. The curves obtained with PGA_{rel} are intermediate between the other two and this choice was considered more suitable for the representation of the actual structural response.

3.4. Results and comparisons of fragility curves developed by the RUs

The consistency of the trend estimated across the approaches with respect to age or height class will be further discussed in Section 4.2. Here, the focus is on the agreement regarding the parameters which define the fragility curves.

Fig. 4 shows the comparison of fragility curves obtained for URM school buildings with two stories and small area (< 500 m^2) belonging to three different ages of construction (namely before 1920, 1921–1945, and 1946–1960).

In particular, the median IM value (i.e., PGA_{DLi}) shows a good agreement for DL1 and DL2 while difference tends to increase for higher DLs. Even in other areas of URM civil engineering research—such as the "URM nonlinear modelling - Benchmark project" [109] aimed at comparing nonlinear modelling approaches of the existing URM buildings—significant epistemic uncertainties have emerged, despite substantial efforts by researchers to standardize assumptions. For example, within this project, it has been shown that while it is possible—by adopting consistent assumptions—to significantly reduce dispersion in the estimation of stiffness and base shear of pushover curves (by approximately 15–20 %), it is not possible to drastically reduce dispersion in ultimate displacement (with dispersion in some cases exceeding 60 %). This result is somewhat consistent with that obtained in the MARS-School fragility curves, i.e. that dispersion for URM fragility curves increases for higher DLs (mostly affected by possible differences in displacement capacities) while is limited in the case of DL2 (mainly related to the capacity of the model to predict the maximum base shear). This consideration may partially contribute to explain the differences especially between mechanical-analytical and hybrid models, which, however, are rather limited overall. In some cases, differences are not null even within the same methodological approach, as for example for empirical and heuristic methods. Concerning the UniCAM curves, it is worth remembering that the response model was inferred from available real data, that were limited to seismic intensities PGA < 0.35 g. Consequently, results concerning larger intensities are extrapolated. Moreover, the dataset mainly included schools retrofitted after the 1997 Marche-Umbria Earthquake and they are expected to be more resistant than schools considered in the other datasets: that may especially explain the difference in DL1 and DL2 compared to the other curves. Furthermore, a slightly different damage metric, correlated to the retrofit costs [69], is used instead of that with the EMS-98 scale [57]. Specifically, the damage index for each building has been derived by UNICAM from data contained in the AeDES survey form [110] which is the same input used by the UNINA and UNIGE research groups for developing fragility curves for the Abruzzi building stock. These data need to be combined to define an overall damage level. The UNICAM group applied a combination rule based on weight coefficients detailed in the work of [69], which have been calibrated to achieve the best fit with data on repair and retrofit costs available in literature ([111,112]). Further details on the comparison between UNIGE and UNINA fragility curves derived for Abruzzi school building stock may be founded in Ref. [66].

Concerning the dispersion of fragility curves, even greater differences are found. On that, it is worth highlighting that the curves provided by UniTS intrinsically consider only the contribution to the inter-building variability; in fact, they analyzed a specific stock of buildings and then they grouped the results of these "as is" configurations on basis of the correspondence between their original features and the classification adopted in the MARS school taxonomy. Conversely, all the other methods – although through different approaches – include the effect of uncertainty related to capacity, record-to-record variability, and DL definition. That justifies the fact the dispersion associated with the UniTS curves is lower than other ones especially for the highest level. In the case of UniCAM curves, as previously mentioned, this may be due to the limited statistical robustness of the sample, particularly for high intensity values.

Fig. 5 shows the comparison of fragility curves for RC school buildings, again for sub-types associated with 2- and 3-stories and small areas; the curves refer to the age of construction after 1976. The figure also highlights the possible impact of gravity (GD) and seismic (SD) design on the seismic vulnerability.

Results appear even more scattered than in the case of URM school buildings, even if a method belonging to the same approach is considered.

In general, results delivered by EUCENTRE provide values of PGA_{DLi} higher than all other approaches (especially for DL1 and DL2), and also highlight a more significant impact of design rules adopted, i.e. if gravitational or seismic. It should be emphasized that, although the methods correspond in terms of approach type, each method is characterized by its own calculation model. For instance, EUCENTRE's model calculates damages for DL3 and DL4 numerically while it defines DL1, DL2 from DL3, and DL5 from DL4 through a calibration process based on observed damage data. This calibration applies a best fit procedure between numerically calculated scenarios and observed damage. The mechanical method POST employs the damage descriptions of building components from the EMS-98. It employs IDR ratios to depict damage patterns for both infills and RC elements across the five damage levels introduced by EMS-98. IDR values for infills come from Ref. [80], while for RC elements, they consider the flexural behavior and potential shear failures. It's worth noting that individual infill panel failure corresponds to DL3, after which the analysis focuses only on RC elements. Given the mechanical basis of the method, IDR values are carefully selected to characterize the onset of damage patterns. This circumstance could potentially lead to conservatism in the results, particularly when compared to empirical methods.

Additionally, results from the empirical and heuristic approaches based on school buildings from L'Aquila are associated only with the seismic design rules. Since L'Aquila has been classified as seismic-prone since 1915, the observed data reflect structural features that account for the consideration of some horizontal forces in the design, though these may not necessarily consistent align current codes. As far as the empirical approach adopted by UniNA and UniCAM is concerned, it is worth recalling that results refer to a different building stock (i.e. that was hit by the L'Aquila 2009 earthquake and the Central Italy 2016–17 earthquake). In general, results

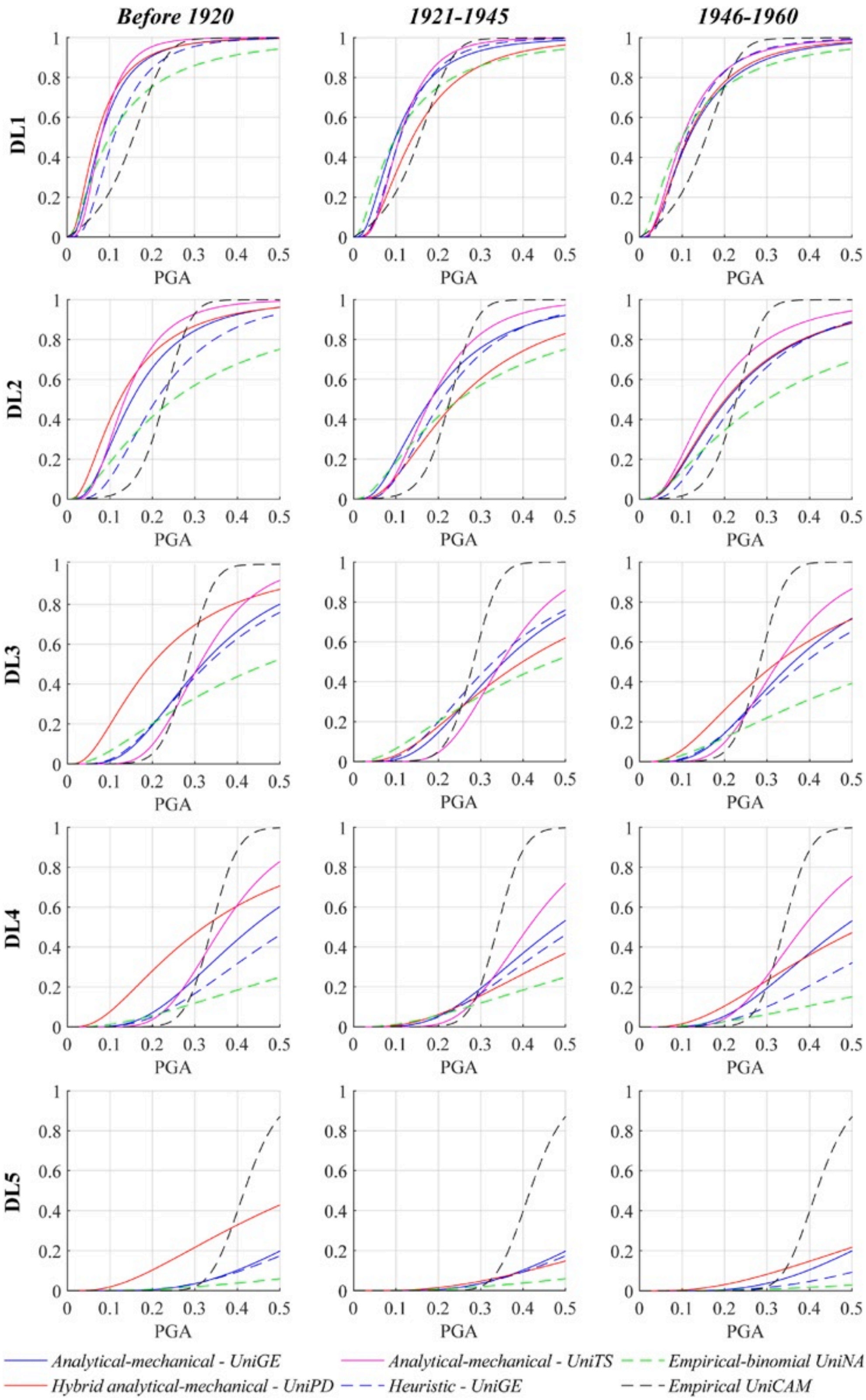

Fig. 4. Comparison of fragility curves provided by research units for URM school buildings.

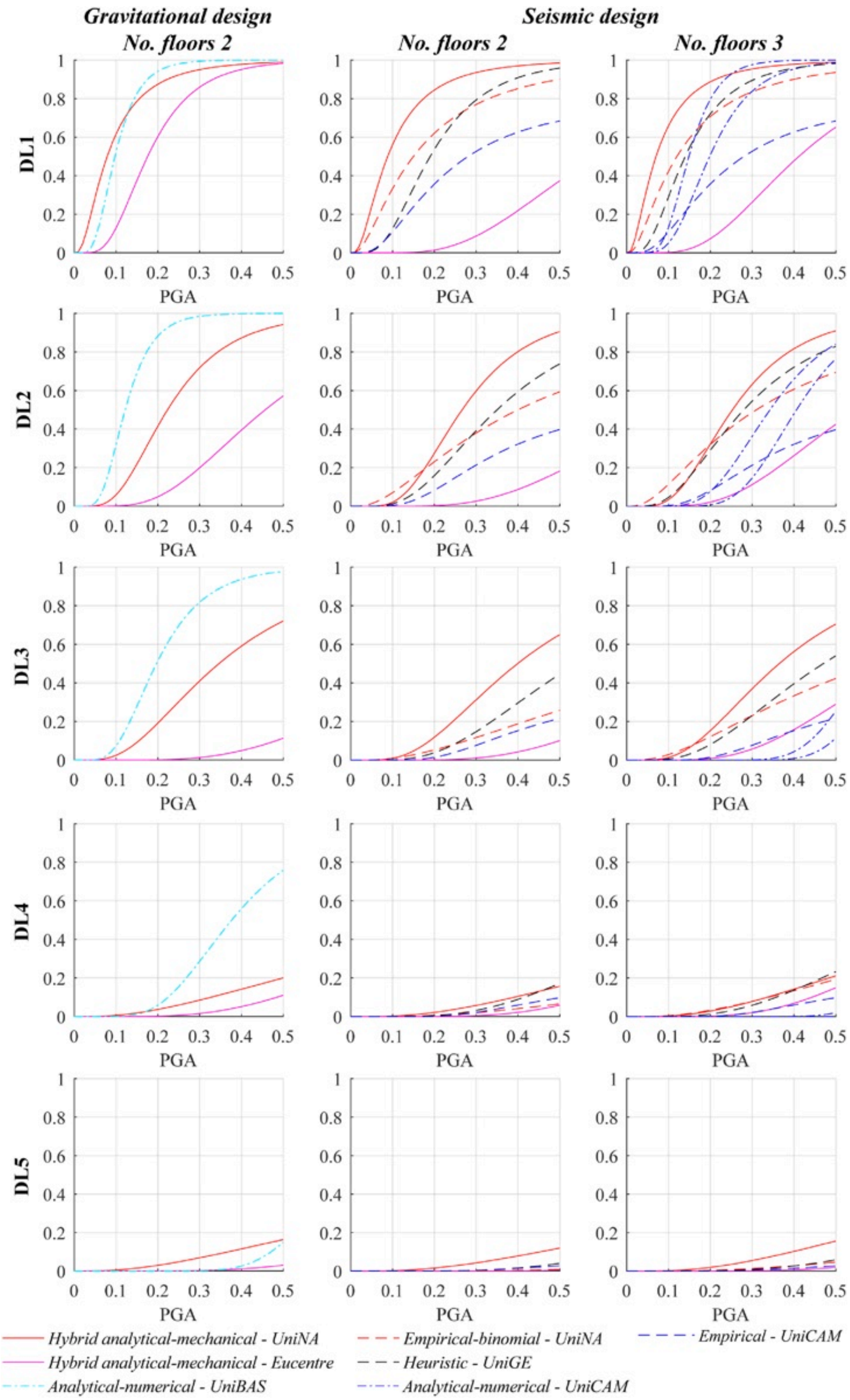

Fig. 5. Comparison of fragility curves provided by research units for RC school buildings (age of construction after 1976).

achieved of UniCAM highlight a building stock less vulnerable; however, this outcome cannot be conclusive since different approaches have been adopted to fit the observed data and a different metric of damage has been adopted, as previously mentioned also for URM school buildings. Both aspects that may influence the final result as discussed in depth in Ref. [66], especially when the number of items into the database is scarce. These aspects are ongoing to be further investigated. Finally, as far as the dispersion is concerned, the curves defined by NLDA directly account only for the record-to-record variability, justifying the lower value obtained.

Even if the differences are not yet negligible in all cases (particularly for certain sub-types and levels of damage), such fragility curves highlight lower dispersions than other comparison available in the literature derived without a such detailed and synergistic work but apparently referring to similar sub-types [113]. Many factors contribute to the differences still remaining in the curves derived by RUs, and at the current state of research, it is not possible to further reduce some uncertainties in their knowledge, one among all is that regarding the complete consistency of damage level definition criteria. However, such a result and the related effort in obtaining it appear a valuable outcome for the scientific community to increase the awareness on the epistemic uncertainty associated with using different approaches to derive fragility curves.

4. The "School-MARS model"

4.1. Basic assumptions to integrate the fragility curves obtained by RUs

The results presented in Section 3.4 demonstrate the extensive and detailed data available from RUs. However, utilizing this data for national-scale seismic risk assessment requires its integration in a synergistic and appropriate manner. To this aim, the development of the unified consensus-based "School-MARS model" introduces several additional challenges, including:

i. defining rules to extrapolate results from RUs when data is partially incomplete with respect to the sub-types required to represent the entire school building stock;
ii. standardizing the contributions of uncertainty and ensuring consistency in the dispersion of the compared fragility curves;
iii. establishing procedures for integrating all available fragility curves into a unified model for each structural type.

The first aspect mainly pertains to the fragility curves developed for RC school buildings, specifically:

- those derived from NLDA, which at the current stage of the research, have been developed considering 7 archetypes. This number is still insufficient to capture the vast inter-building variability characterizing the multifaceted Italian building stock. The limited number of archetypes is due to the high computational burden of this approach, coupled with the necessity for highly accurate data on archetypes;
- those obtained from the empirical or heuristic methods, which – due to the specific features of the real building stock examined – are deemed more representative of structures with low to medium seismic design and, consequently, less vulnerable than the expected performance of buildings designed primarily for gravity loads.

The combination of sub-types with a different number of curves may introduce inconsistencies in the results, not due to genuinely possibly contradictory predicted behaviours but rather due to an ineffective combination phase. To address this, appropriate criteria have been adopted, leveraging trends observed in other approaches or other building stocks that are statistically more robust, like the residential one discussed in Ref. [40].

Regarding the second issue, deterministic values from literature, consistent with the considered types of uncertainties, have been combined with those directly available from the various methods adopted (i.e. the record-to-record variability from NLDA and the inter-building variability from UniTS approach). The combination was performed using the square root sum of the squares (SRSS) rule.

After addressing these issues, and to enable a more effective comparison not only within the school building stock but also between it and the residential stock, the fragility curves originally derived by the RUs were converted as initially proposed in the MARS project ([114,115]). This method allows the conversion of the fragility curves associated with each DL into percentages of vulnerability classes. Specifically, six vulnerability classes have been considered with the aim of being consistent with those of the EMS-98 scale, ranging from A (most vulnerable) to F (least vulnerable). According to the proposal of [115], a set of five fragility curves - associated to the EMS98 classes and still in accordance with a lognormal format - is defined by the following parameters: the median value of damage level DL2 (PGA_{DL2}); the ratio PGA_{DLk}/PGA_{DL2}, related to the median values of PGA for the other damage levels ($k = 1,3,4,5$); and the dispersion β_{Dk} (assumed in this application equal to 0.65). The value PGA_{DL2} is assumed as reference being representative of a moderate-slight structural damage, close to the reaching of the maximum shear strength. The ratio PGA_{DLk}/PGA_{DL2} introduces a relevant concept, intrinsically related to the "ductility" (or better "behavior factor") in the case of DL3, DL4 and DL5. It allows to differentiate brittle and ductile behavior taking into account the possible variation in the spacing between fragility curves associated to DLs. Two sets of fragility curves, named "brittle" and "ductile", have been proposed in Ref. [115] through different reference values for the PGA_{DLk}/PGA_{DL2} ratio. Conversely, the value PGA_{DL1}/PGA_{DL2} expresses the overstrength ratio in URM buildings while is mostly related to the damage of infill and partition walls in RC buildings.

Tables 6 and 7 summarize the values of PGA_{DL2} and the ratio PGA_{DLk}/PGA_{D2}. The PGA_{DL2} values reflect the EMS98 assumption that the difference between one vulnerability class and the next is that an increase of one degree in macroseismic intensity is required to achieve the same level of damage. Values of Table 6 are consistent with the common format of PGA-I correlation laws [116,117], i.e. $PGA = c_1\, c_2^{I-5}$ (where c_1 represents the PGA for intensity $I = 5$, while c_2 is the factor of increase of PGA due to an increase of one of the macroseismic intensity). Values of Table 6 correspond to the adoption of c_1 and c_2 respectively equal to 0.047 and 1.8. The plausibility of the values proposed in Tables 6 and 7 has been also confirmed by the in-depth comparison made within the

Table 6
Reference values of PGA_{DL2} established in Ref. [115] for applying the conversion of fragility curves into vulnerability classes percentage according to the MARS metric.

Vulnerability classes	A	B	C	D	E	F
PGA_{DL2} [g]	0.11	0.20	0.36	0.64	1.16	2.09

Table 7
Reference values ratio of the PGA_{DLk}/PGA_{DL2} established in Ref. [115] for applying the conversion of fragility curves into vulnerability classes percentage according to the MARS metric Note that for DL1, two different values have been considered for URM and RC types.

PGADLK/PGADL2	DL1 (URM)	DL1 (RC)	DL2	DL3	DL4	DL5
Brittle	0.67	0.57	1	1.49	2.23	3.32
Ductile	0.51	0.39	1	1.95	3.82	7.46

Italian National Risk Assessment made in 2028 (NRA 2018 - [41,60]). Moreover, the trend of values summarized in Table 7 can be analytically expressed as:

$$\boldsymbol{PGA_{DLk} = PGA_{DL2} e^{\alpha(k-2)} \quad k = 1, \ldots, 5} \tag{1}$$

where the factor α is a free parameter that ranges between 0.36 and 0.66, moving from the maximum brittle to ductile behavior. Moreover, this parameter can be also useful to distinguish the behavior variation introduced by retrofitting interventions (as shown for example in Ref. [118]).

As a consequence, based on the general framework introduced in Ref. [115] and previously mentioned in a concise manner, a set of five fragility curves can be represented equivalently by either a pair of values, namely PGA_{DL2} and α, or by a set of vulnerability class percentages (specifically, 12 values: 6 for describing the rate of ductile behavior and 6 for the rate of brittle behavior).

To convert the fragility curves proposed by the UR into vulnerability class percentages, the free parameters PGA_{DL2} and α (Eq. (1)) are defined through a least-squares regression of the percentage error between the MARS reference fragility curves (Tables 6 and 7) and each UR curve. This method also implies identifying the two contiguous vulnerability classes between which the determined PGA falls. Finally, a linear interpolation in the logarithmic plane is used to determine the percentages associated with the vulnerability classes. Further details on the conversion procedure are provided in Ref. [115].

Once the fragility curves have been converted, their integration becomes straightforward and easy. For example, under the hypothesis of assigning an equal weight to each approach, a simple average of the vulnerability class percentages can be calculated.

Differences in ductile/brittle percentages are expected depending on the construction age, since buildings are characterized by different structural details or seismic regulations adopted during design. Consequently, this will result in varying percentages of "ductile" and "brittle" vulnerability classes.

The result of such a conversion - when applied to the fragility curves presented in Section 3.4 (after the homogenization in terms of uncertainty sources accounted in the dispersion) - is illustrated in Section 4.2.

4.2. Definition of the unified "School-MARS model"

The final unified "School-MARS model" has been defined by the combination of a total of five models for each structural type. For both URM and RC school buildings, two models belong to the *empirical* (by UniNA) and *heuristic* (by UniGE) approaches. The other three belong: for URM school buildings, to the purely *mechanical-analytical* (by UniGE and UniTS) and *hybrid* (by UniPD) approaches; for RC school buildings, to the *hybrid* approach by UniNA and EUCENTRE and to the *mechanical-numerical* one from NLDAs (in this case, all results provided by various RUs were firstly merged). Since the empirical fragility curves developed by UniCAM assumed some alternative damage metrics, it has been decided to not include it in this comparison at this state of the research.

The combination was made under the assumption of assigning the same reliability weight to each method. This assumption has been made because, as reported in Sections 3.1.1-3.1.4, at this stage of the research none of the approaches can be considered significantly more reliable than the others and each vulnerability model has its own advantages and drawbacks. Moreover, also results illustrated in Section 4.3 confirm the liceity of such an assumption.

Fig. 6 shows the results in terms of the percentage of vulnerability classes as provided by adopting the MARS conversion procedure [115]. From the graphs in which the results of single RUs are reported (Fig. 6a/c), it emerges a greater dispersion of results for RC school buildings than the URM ones, as already highlighted by the comparison of the fragility curves originally developed by RUs. Instead, the graph to Fig. 6b/d shows the percentage of vulnerability classes as resulting from the combination of the five approaches.

Finally, it is worth highlighting that such combination procedure preserves the evidence on differences among RUs results but, at the same time, allows to interpret the individual result under the same hypotheses' umbrella.

Such an approach appears suitable also in making the comparison across different structural types and various sub-types. To get an overview of the results obtained from the unified MARS-Schools model, some of the results are shown in the figures below (Figs. 7–10) by varying building types (URM or RC), age of construction, number of storeys and design level (GD or SD).

Regarding the variation in the age of construction, Fig. 7 shows, for URM schools, a shift of behaviour from class B to class C moving from older to modern eras. Such a result is mainly ascribable to the change in the effectiveness of structural details with the age of

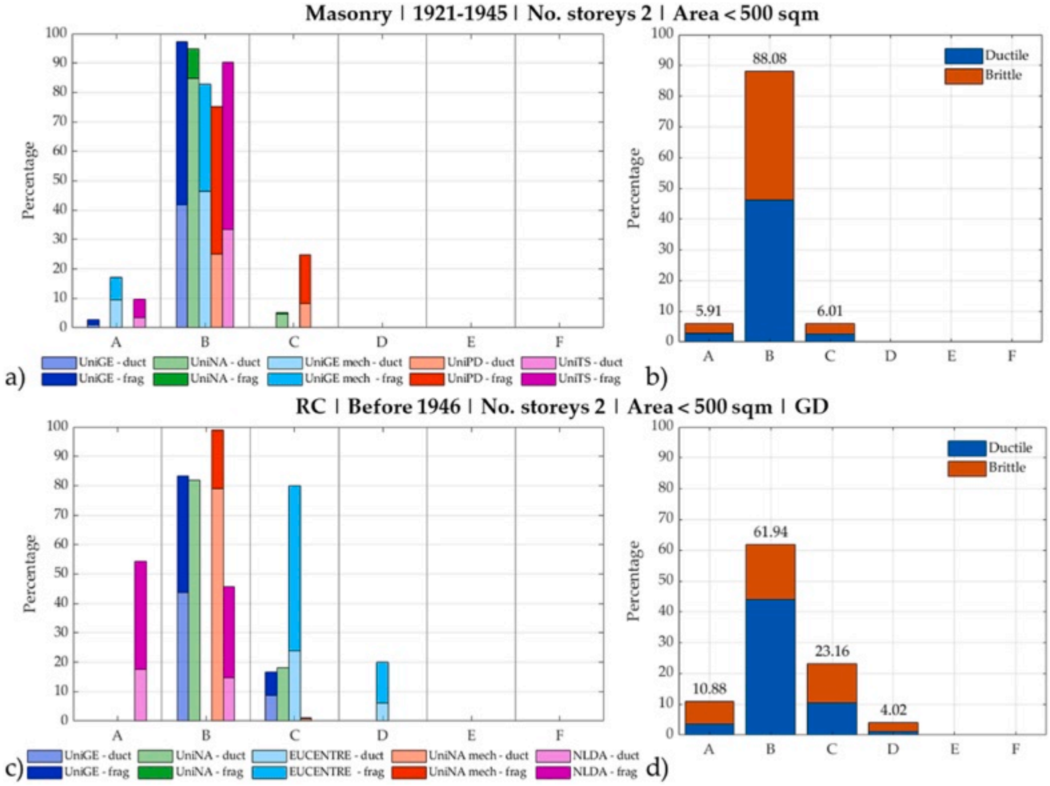

Fig. 6. Distribution of vulnerability classes obtained from research units and the integrated MARS-Schools model, for masonry and reinforced concrete schools.

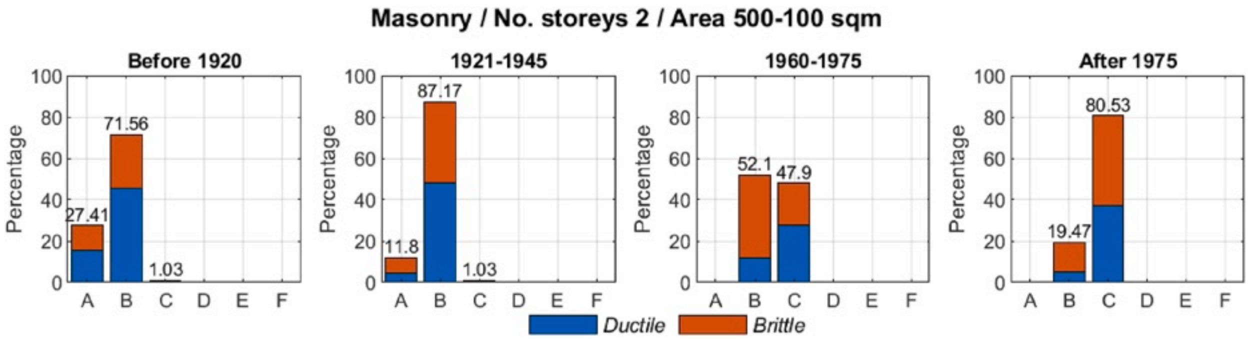

Fig. 7. Distribution of vulnerability classes of the unified MARS-Schools model by varying the age of construction. Results refer to URM schools with 2 storeys and area 500–1,000 sqm

construction. Specifically, it moves from a dominant presence of weak spandrels configuration before 1920 (which makes the building also more prone to out-of-plane mechanisms) to a predominance of RC beams or tie-rods coupled to spandrels in modern era (which makes the building consistent with the box-type behaviour assumption).

In the case of RC, it is the design rule adopted – if seismically (SD) or gravitationally (GD) designed, to primarily affect the seismic response. Indeed, in the right-hand side of Fig. 8 (gravitational design), no substantial differences in the behaviour emerge varying the age of construction (i.e. if before or after the 1976), while it is evident in the seismic design by comparing before and after 1976. In the case of RC buildings, the transition between pre and post 1976 is crucial since significant changes in the seismic load modelling were introduced by the Law 02/02/1974 and the Ministerial Decrees DM March 03, 1975, in terms of seismic design provisions and of seismic classification of each municipality. In fact, as debated in Section 2, DM March 03, 1975 introduced for the first time in Italy some basic earthquake engineering concepts.

Figs. 9 and 10 show the variation in structural behaviour as the number of storeys changes, respectively for URM and for RC school buildings. This comparison is carried out by fixing the age of construction (1921–1945 for masonry schools and after 1976 for RC). The graphs show, for both types of construction, a strong dependence of seismic vulnerability as the number of storeys varies, and specifically an increase in vulnerability as the number of storeys increases.

Figs. 11 and 12 show the results obtained from the MARS-Schools model in terms of vulnerability classes as the plan areas change.

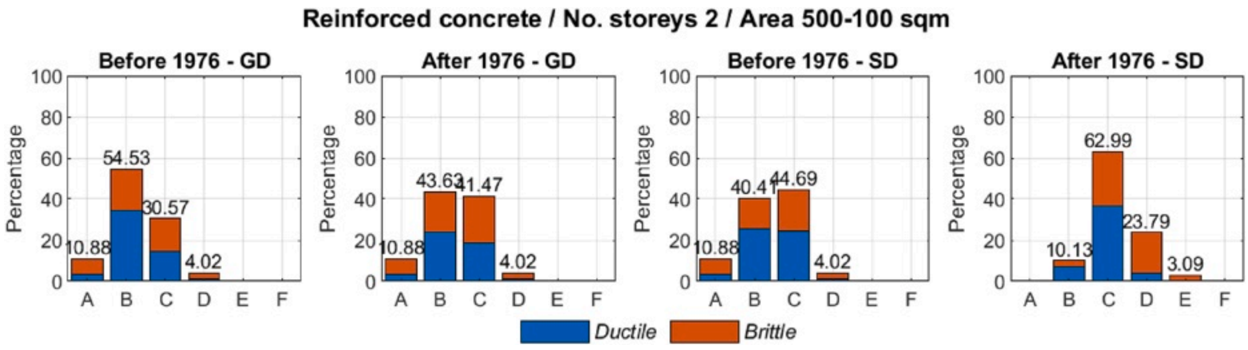

Fig. 8. Distribution of vulnerability classes of the unified MARS-Schools model by varying the age of construction variations. Results refer to RC schools with gravitational design (GD) or seismic design (SD), having 2 storeys and area 500–1000 sqm

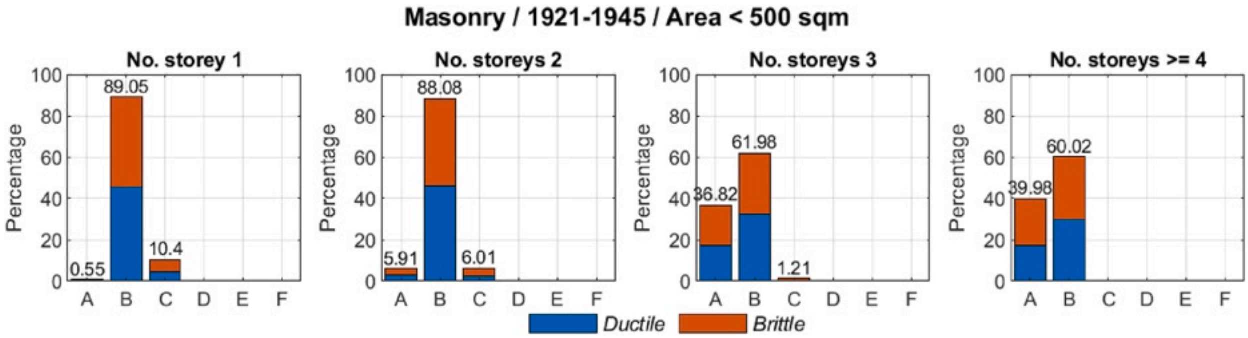

Fig. 9. Distribution of vulnerability classes of the integrated MARS-Schools model as the number of storeys variations, for masonry schools.

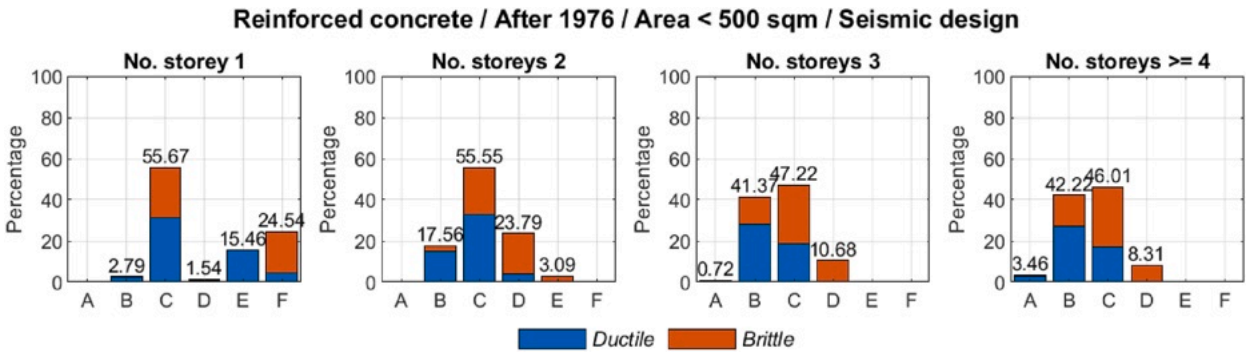

Fig. 10. Distribution of vulnerability classes of the integrated MARS-Schools model as the number of storeys variations, for reinforced concrete schools with seismic design.

The results show a little dependence of the model varying plan areas, for RC school buildings, while a slightly greater sensitivity, for URM school buildings, when the plan area is $> 1{,}000$ m^2. This result may be explained by the greater plan form irregularity that characterizes masonry buildings with higher plan areas. Additionally, at this stage of the research, not all models used in the project are able to consider the difference in plan area. An example includes the empirical models where the scarcity of items in the database has prevented further subdivision of sub-types to estimate trends in the vulnerability with different plan area. The complete set of fragility curves of the "School-MARS model" is provided in the paper as Supplementary Data. Please note that, in general, the dispersion values (β_{Dk}) are slightly higher than 0.65, and vary across the sub-types, as the final values also account for the model epistemic uncertainty, explicitly considered through the use of five different approaches.

4.3. Validation of the MARS-school model

A first validation of the MARS-Schools model was performed using the data of damage observed on public school buildings hit by the 2009 L'Aquila earthquake. This information is available thanks to the ReLUIS consortium that supports the ICPD in post-event surveys and usability assessment. In Ref. [66], Damage Probability Matrices (DPM) were defined from the damaged framework compiled in the AeDES form [110] associating to each school: the damage grade through a conversion rule based on a peak approach conceived

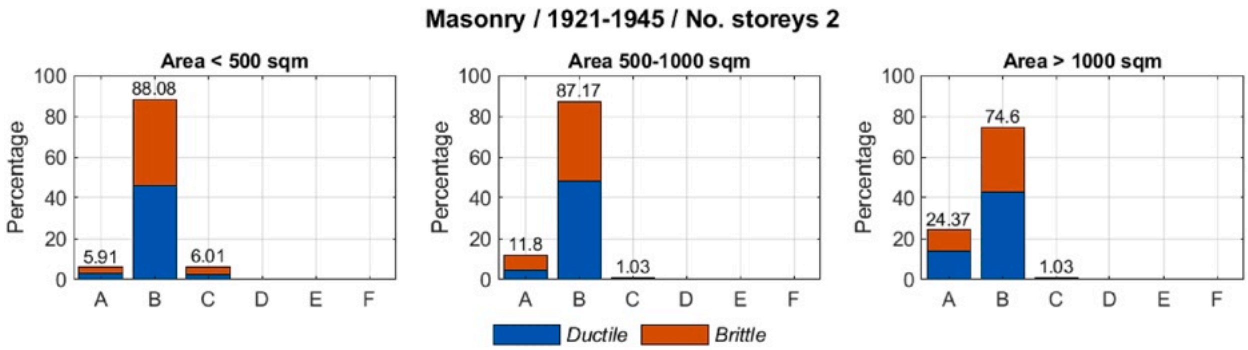

Fig. 11. Distribution of vulnerability classes of the integrated MARS-Schools model as the plan area variations, for masonry schools.

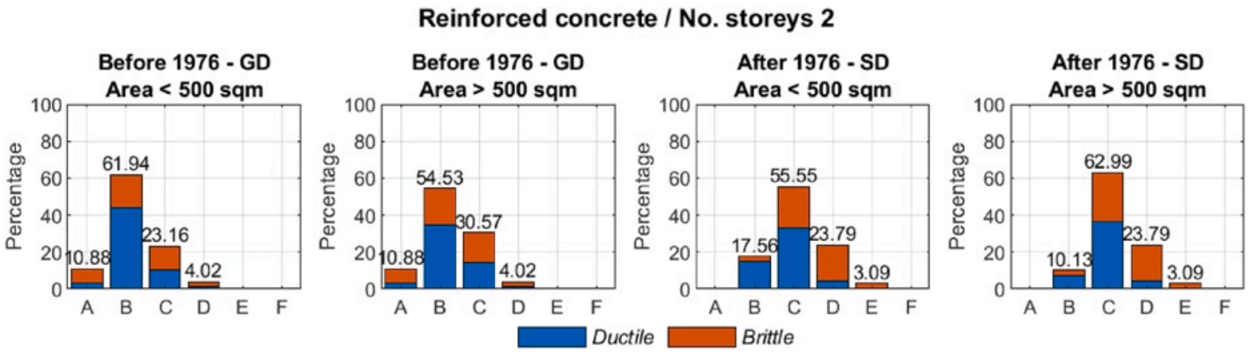

Fig. 12. Distribution of vulnerability classes of the integrated MARS-Schools model as the plan area variations, for reinforced concrete schools with gravitational design (GD – Before 1960) and whit seismic design (SD – After 1960).

to be consistent to the EMS-98 scale [57]; and the PGA value that hit each school. The shakemaps used to associate the PGA value to each individual building are based on the procedure described in Ref. [119].

Fig. 13 shows the spatial distribution of PGA values at the site location, which are determined as the maximum value between the main shock and related aftershocks (i.e. April 7, 2009 Mw 4.8, April 7, 2009 Mw 5.3, April 9, 2009 Mw 5.1, April 9, 2009 Mw 4.9).

Fig. 14 illustrates the comparison between the DPM estimated alternatively by the MARS-school model (a/b) or each individual model (c/d) and the one assessed from real observed data according to Ref. [66]. Specifically, the latter is depicted by a black line [66] while the bars are the results obtained with the MARS-Schools model, i.e. by characterizing the sub-typology of each school in the sample and entering the fragility curves with the PGA associated. The graphs show the damage levels from DL0 to DL5 in the abscissa, while the ordinate shows the probability of attainment of each damage level. The comparison in Fig. 14 considers the overall sample from the affected towns of the Abruzzo region, that comprises 1,330 RC schools and 692 URM schools.

Similarly, Fig. 15 shows the comparison considering only the structures present in the city of L'Aquila, where the epicenter of the seismic event occurred. Both scales, i.e. that of the whole region or that of municipality of L'Aquila, are relevant for the validation aim, since they allow to check the capability of the model to correctly estimate varying different damage levels, from low-to-medium in the area far from the epicenter to very severe, like that expected in the crater.

Overall, the results show a very good consistency between observed and calculated damage using the unified MARS-Schools model. Although some methods were calibrated using observed data, the overall result was by no means guaranteed. From Fig. 14c, it can be observed that only one model, specifically the EUCENTRE model for RC schools, tends to slightly underestimate the damage. However, overall, this model also performs well. Given that the primary focus of the paper is on a large national scale, these results are considered satisfactory. There were no strong reasons to assign different weights to the individual models, thus confirming the validity of the assumption introduced in Section 4.2.

5. Risk assessment at national scale

The MARS-Schools vulnerability model has been incorporated into an online platform, named IRMA (Italian Risk MAps) [120], able to perform risk analyses for different assets according to the common probabilistic approach [121]. As better described below, seismic risk (in terms of estimated damage distribution) is assessed through the convolution of three main parameters, i.e. exposure (consistency and attributes of the asset at risk), seismic hazard (expected ground motion intensity in a certain interval of time at a site) and vulnerability (expected physical damage of an asset as a function of a given intensity measure). Starting from damage distribution, physical damage-consequence functions are used to obtain risk results in terms of direct economic losses, unusable buildings (in the short and long period) and casualties (injured and deaths). According to the terminology introduced in Ref. [122], different

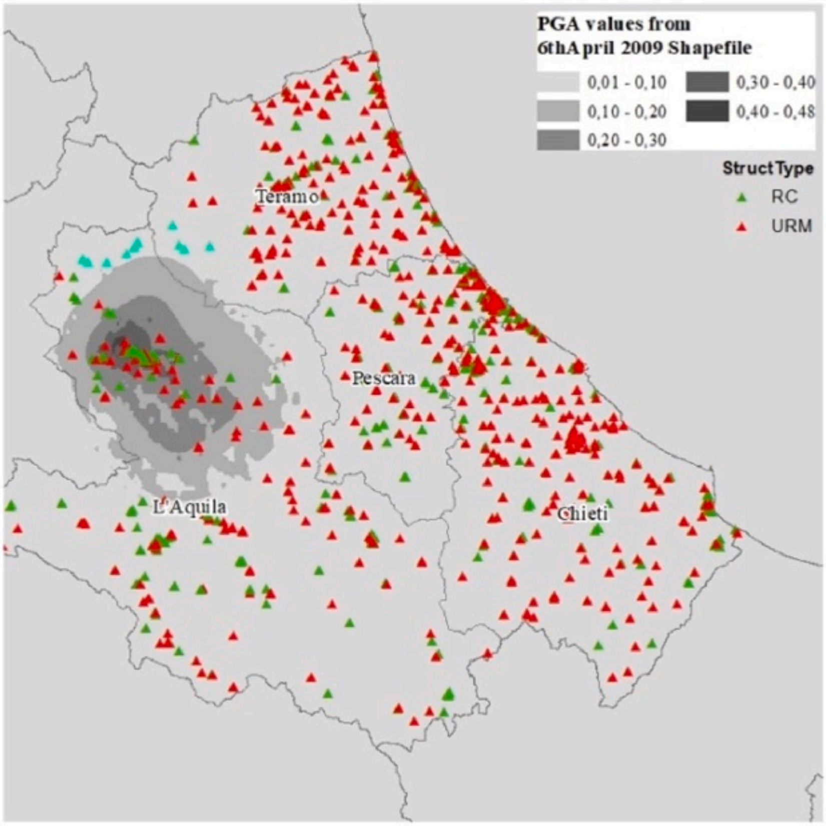

Fig. 13. Shakemaps illustrating the PGA values associated with each building in the school stock hit by the 2009 L'Aquila earthquake. In green the RC school buildings and in red the URM ones; school buildings indicated by light blue colour are those for which the maximum PGA was attained in an aftershock. (For interpretation of the references to colour in this figure legend, the reader is referred to the Web version of this article.)

types of assessments were carried out, namely: intensity-based risk, i.e., by considering seismic intensities related to events having a selected return period; or time-based risk, i.e., by considering all events expected in an observation time window.

In the following, the main features of the IRMA platform are described (Subsection 5.1). Therefore, in Subsection 5.2, the current results are illustrated in terms of expected damage distribution and usability rating. They were obtained by considering: the *exposure* data from the Italian school buildings inventory set up by the Ministry of Education in 2005 (see Section 2.2); the *seismic hazard* introduced by the MPS04 seismic hazard model ([123,124]), developed by INGV (National Institute of Geophysics and Volcanology), along with the soil amplification map provided by Ref. [125] for the entire Italian territory; and the MARS-Schools *vulnerability* model. Losses in terms of usability rating are estimated through specific damage-consequence functions based on the data from the reconstruction process after L'Aquila 2009 earthquake [111].

5.1. The IRMA platform for school buildings

IRMA (Italian Risk MAps) [120] is an online platform developed by the EUCENTRE, in close collaboration with ReLUIS, for the ICPD. It is intended for the scientific community to generate risk maps and damage scenarios according to consensus models.

The computational engine of IRMA is OpenQuake [126] whose components have been fully integrated into the platform. The platform consists of several tools for different assets, one of these dedicated to the seismic risk assessment of school buildings, named "IRMA Schools" [56]. It is flexible and allows the user to create and, then, upload different exposure matrices and different sets of fragility curves and combine them. The only two fixed elements are the exposure database and the seismic hazard model. The exposure pre-loaded database is the Inventory of Italian schools provided by the Ministry of Education and described in Section 2.2. The seismic hazard model is the MPS04 map ([123,124]), adopted on a national level by Civil Protection Ordinance [127] and by the New Technical Standards for Construction ([53,54]). For the evaluation of local amplification effects in IRMA Schools, the shear wave velocity at 30 m depth (V_{s30}) map developed by Ref. [125], with a grid of 50 m by 50 m, was included. The homepage of the platform is presented in Fig. 16.

The two key elements that users define and upload to the platform are the exposure/vulnerability matrix and the set of fragility curves that jointly describe the seismic behaviour of school buildings. The exposure/vulnerability matrix allows the user to select from drop-down menus the characteristics that define the taxonomy of school buildings. The behaviour of sub-types is defined ac-

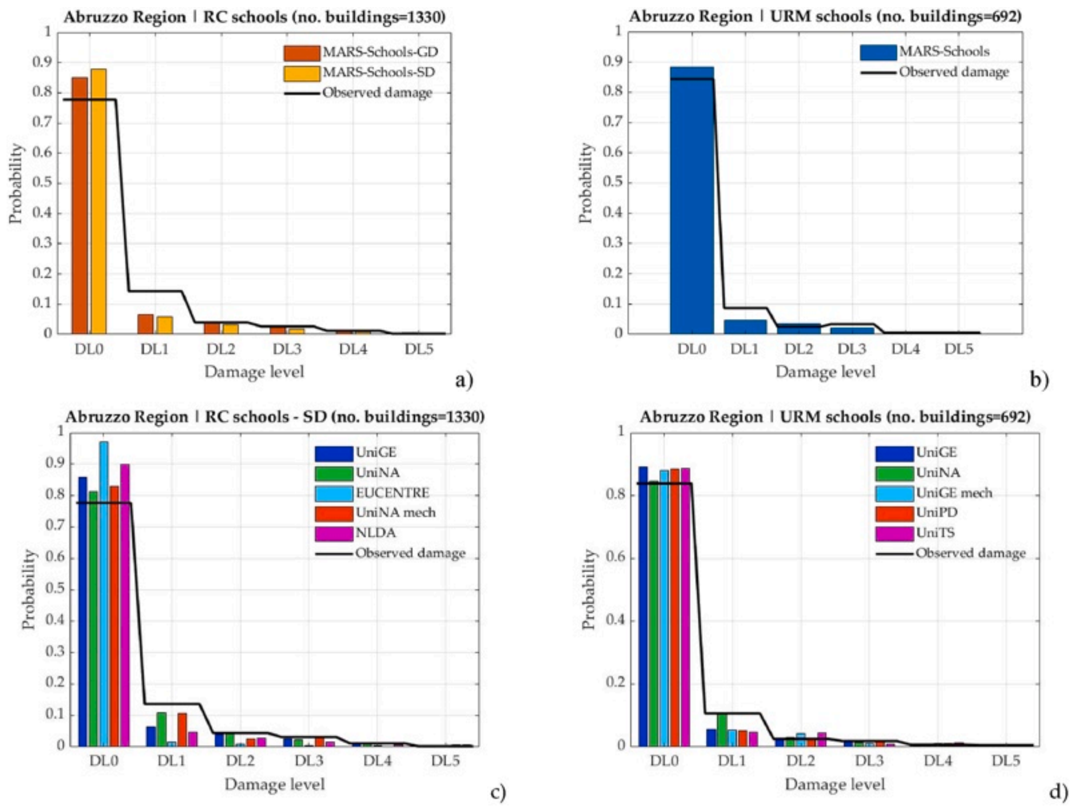

Fig. 14. Simulation of the damage scenario with the MARS-Schools model and with each individual model to carry out a validation with the data of schools hit by the 2009 L'Aquila earthquake. RC (a/c) and masonry (b/d) schools from all the affected towns of the Abruzzo region are respectively reported for the MARS-Schools model (a/b) and the individual models (c/d).

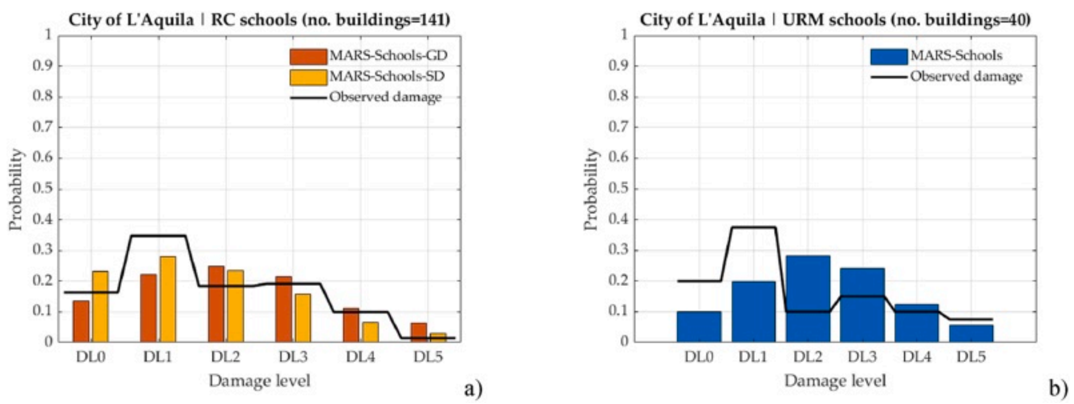

Fig. 15. Simulation of the damage scenario with the MARS-Schools model and validation with the data of schools hit by the 2009 L'Aquila earthquake, for RC (a) and masonry (b) schools in the city of L'Aquila.

cording to the taxonomy introduced in Section 2.2. and described using a combination of the twelve vulnerability classes introduced in Section 4.2 (e.g. A-ductile, A-brittle, B-ductile, B-brittle).

The expected damage levels are five, in accordance with the EMS-98 [57], from DL1 (light damage) to DL5 (collapse). Fig. 17 shows the logical scheme of the platform: in blue the preloaded fixed elements and in green the variable elements that the user has to fill in and load.

Once these two elements have been defined and uploaded, the user can start the calculation:

- by selecting the Region of interest (a specific one or all of Italy);
- by running the calculation on rock or considering soil amplification;
- by selecting the type of analysis, choosing between intensity-based damage (for specified return periods) or time-based damage (for time windows of 1, 10, and 50 years).

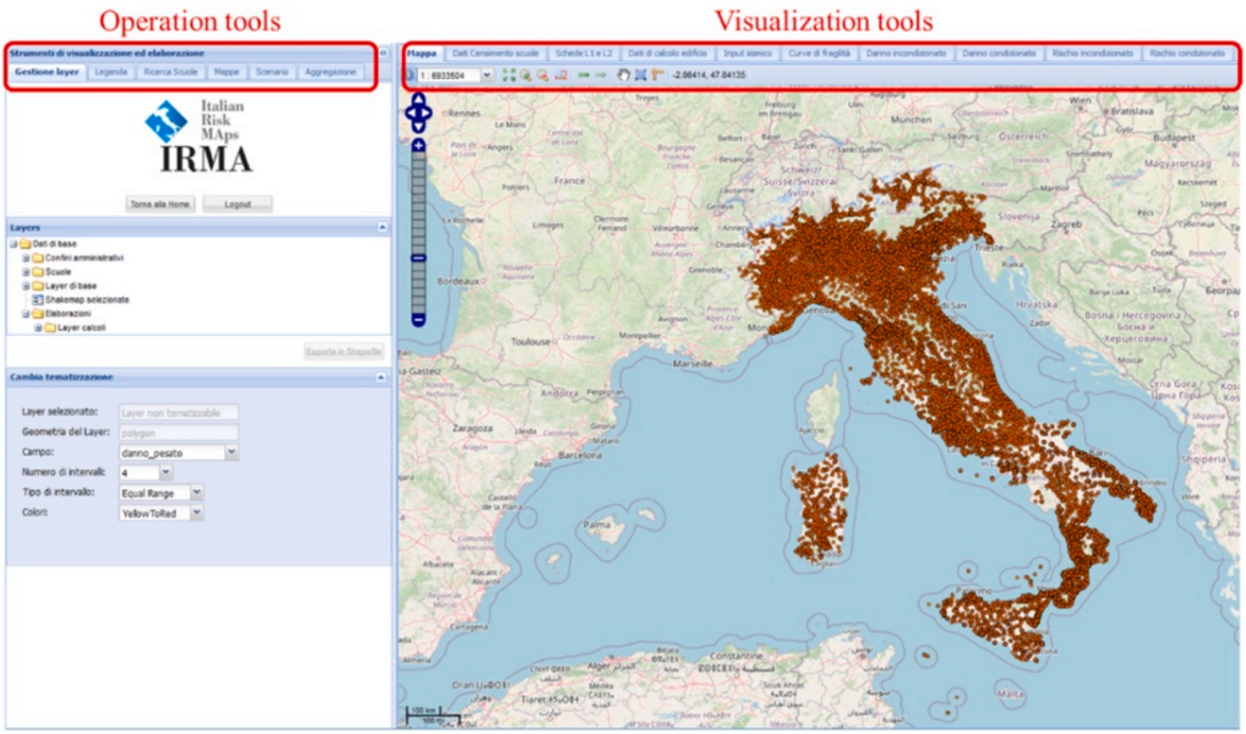

Fig. 16. Homepage of the IRMA Schools Web platform. Orange dots refer to school buildings collected in the inventory provided by the Ministry of Education. (For interpretation of the references to colour in this figure legend, the reader is referred to the Web version of this article.)

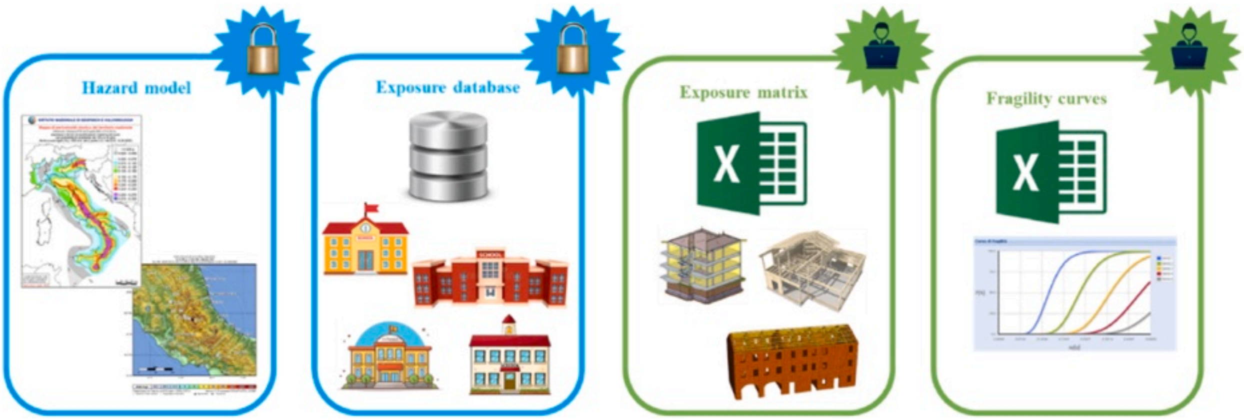

Fig. 17. Logical scheme of the IRMA School platform.

Three levels of visualization of aggregated results are provided: Municipality, Province, and Region. Finally, by combining the results in terms of damage, it is also possible to calculate the risk in terms of economic losses and impact on usability (i.e. Useable, Unusable, and Collapsed), as illustrated in more detail at Section 5.2.

In Italy, the built environment varies significantly from one Region to another due to socio-economic factors and, for older buildings, the availability of construction materials. Consequently, the platform allows for the use of different exposure matrices and sets of fragility curves for each Region or group of regions (e.g., Regions in Central Italy near the Apennines have buildings with similar characteristics). Therefore, results can be aggregated to create comprehensive maps for the entire territory.

5.2. Seismic risk results

The MARS-Schools model has been implemented into the IRMA-School platform [56] to demonstrate its potential for conducting national-scale seismic risk assessments.

The results are specifically focused on RC and URM school buildings, for which the fragility curves and the MARS-schools model presented in the previous sections can be directly applied. Consequently, the maps presented in the following refer only to the sample of schools where the structural material is specified, namely 10,279 for URM (21 %) and 15,323 for RC (31 %). The remaining 48 %

(22,536 schools) corresponds to either “other” structural types or buildings with missing structural material information (see Section 2.2 for the discussion on the completeness of the available inventory).

Fig. 18 shows the maps illustrating the intensity-based mean damage consequent to a seismic input corresponding to 475 years return period. Specifically, Fig. 18a/b/c refers to URM school buildings, while Fig. 18d/e/f to RC ones; the number of buildings associated to each DL is here aggregated at province scale. The Figure reports both results associated to DL2 and DL3 and the mean damage (μ_D, which ranges from 0 to 5) computed from the overall distribution. To relate the μ_D value to a more concise damage concept, a conversion is included in the legend that translates the value into a single discrete damage level. This approach follows the original proposal of [59] which is based on the binomial distribution. The thresholds adopted for such a conversion are defined in the legend of Fig. 18. Note that the areas marked in white indicate provinces where either no schools with the specified construction materials are present or the database lacks data for these materials altogether. Focusing on Fig. 18c/f, it emerges that, apart from a few small Northeastern provinces which exhibit the maximum damage levels (DL3 and DL4, i.e. the brown and yellow areas in Fig. 18c/f), URM school buildings primarily located along the Apennines and in some provinces of Sicily are likely to experience DL2. In contrast, for RC ones, DL2 is expected only in a few provinces.

In the case of schools, results aggregated in terms of plan area are interesting because this parameter can be easily correlated to the number of people attending each school (students, and personnel). This is information potentially very relevant for estimating the expected seismic losses. To this purpose, Fig. 19 shows the intensity-based damage maps aggregated by province in terms of plan area, separately for URM (Fig. 19a) and RC buildings (Fig. 19b).

Similarly to the results presented in Fig. 18, the areas mostly damaged are estimated in some Northeastern provinces while, in the rest of the territory, a prevalence of DL2 is expected, especially in URM schools compared to RC ones. Since the data in terms of plan area are available only for a small number of schools, there are many provinces for which the result cannot be aggregated (areas in white, that in fact increase in number compared to Fig. 18). In addition, note that the IRMA-School platform performs the aggregation only if the data on the plan area reaches a completeness percentage of at least 70 %. This value corresponds to the threshold assumed for the estimate of a reference average value enough robust.

Robust consequence functions constitute the essential requisite to finalize the seismic risk assessment in terms of losses, and profitably exploiting the damage estimate illustrated in Figs. 18 and 19. The availability of the damage observed after the 2009 L'Aquila earthquake event was crucial for calibrating customized consequence functions for the school buildings. At the current stage of the re-

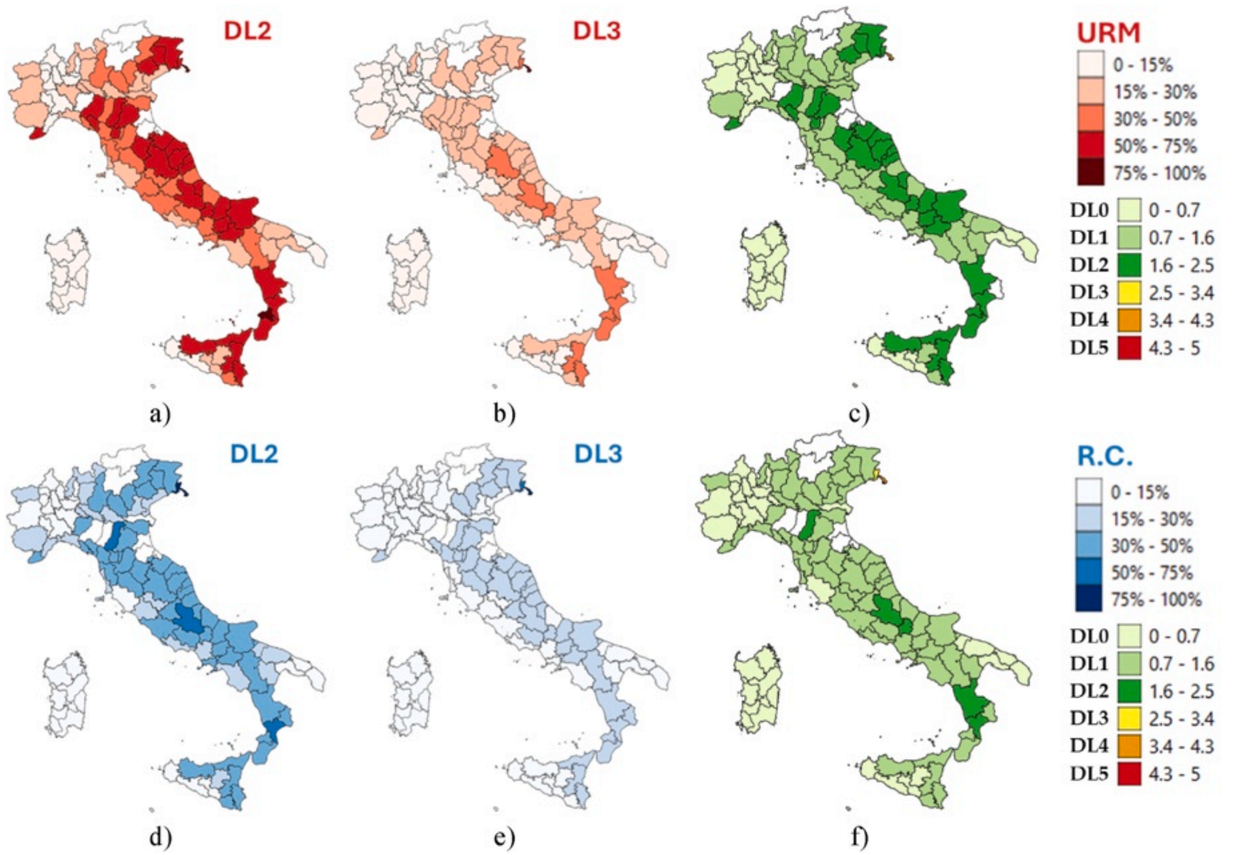

Fig. 18. Intensity-based damage maps with 475-year ground shaking intensity for URM (a) and RC (b) school buildings. Results are aggregated by province in terms of percentage of the number of buildings and refer to DL2 (a/d), DL3 (b/e) and the mean damage mD (c/f).

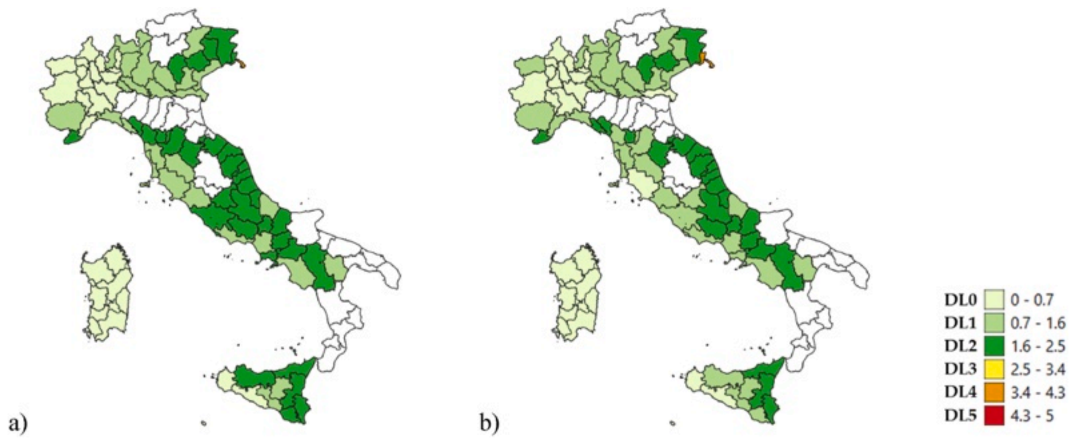

Fig. 19. Intensity-based damage maps with 475-year ground shaking intensity for URM (a) and RC (b) school buildings. Results are aggregated by province and on the plan area.

search, the consequence functions and the related losses were determined only for usability outcomes. Based on data provided in Ref. [66], which correlate the distribution of the usability rating coming from the AeDES forms into DLs, Tables 8 and 9 show the consequences matrices considered for RC and URM school buildings, respectively. Each matrix illustrates the percentage of buildings in terms of “Useable”, “Unusable-short time”, “Unusable-long time”, “Collapsed” usability ratings as a function of the damage level (from DL1 to DL5). For completeness, the values in brackets indicate those adopted for residential buildings in the NRA2018 [41], primarily based on data obtained from the reconstruction process following the 2009 L'Aquila earthquake [111]. Additional details on the criteria used to define such values are provided in Ref. [128].

The consequence matrices defined for school buildings significantly differ from those used for the Italian residential ones ([60,129]), especially in the case of lower damage levels. For example, the consequence matrices for URM school buildings show low percentages of “Unusable long time” at DL1 whereas for residential buildings, this does not occur until DL3. This difference may be ascribable to variations in the intrinsic vulnerability of school versus residential buildings, including that associated with the response of non-structural components. Additionally, it may reflect the influence of other factors on usability judgments for strategic buildings, such as risk perception in filling in the AeDES form, which often leads to assigning more cautious ratings.

Estimates of losses in terms of expected usability for the Italian school buildings are presented in Tables 10 and 11. Results refer to time-based risk analyses and indicate the number of school buildings (and the related percentage over the total number of buildings) for “Useable short time”, “Useable long time” and “Collapsed”. Two time windows have been adopted, 1-year and 50-years respectively reported in Tables 10 and 11.

From the usability results associated to short- and long-time obtained from the risk analyses with 50-years time window, it emerges that approximately 26 % of RC buildings and 31 %, of URM structures would be potentially unusable. For RC buildings, this result primarily depends on damage conditions that can be repaired with short-time countermeasures (approximately 20 %) whereas for URM schools, similar percentages are observed for both short- (15 %) and long-time usability conditions (16 %). Consequently, in terms of expected unusability, URM school buildings would exhibit a higher risk compared to RC structures. On the other hand, for

Table 8
Consequence matrix defined for calculating the losses in term of usability, for RC schools. In brackets the values indicate those adopted in the NRA2018 for residential buildings.

	Useable	Unusable short time	Unusable long time	Collapsed
DL1	65 (100)	35 (0)	0 (0)	0 (0)
DL2	0 (60)	80 (40)	20 (0)	0 (0)
DL3	0 (0)	35 (40)	65 (60)	0 (0)
DL4	0 (0)	15 (0)	85 (100)	0 (0)
DL5	0 (0)	0 (0)	0 (0)	100 (100)

Table 9
Consequence matrix defined for calculating the losses in term of usability, for URM schools. In brackets the values indicate those adopted in the NRA2018 for residential buildings.

	Useable	Unusable short time	Unusable long time	Collapsed
DL1	40 (100)	50 (0)	10 (0)	0 (0)
DL2	0 (60)	33 (40)	67 (0)	0 (0)
DL3	0 (0)	20 (40)	80 (60)	0 (0)
DL4	0 (0)	0 (0)	100 (100)	0 (0)
DL5	0 (0)	0 (0)	0 (0)	100 (100)

Table 10
Usability rating at the national scale from time-based risk analyses considering a 1-year time window. The "Exposure" data refers to the total number of buildings considered and the relative percentage with respect to the entire database (in italic and in bracket).

	Unusable short- time	Unusable longtime	Collapsed	Exposure (no. buildings)
RC	100	20	2	15323
	0.6 %	0.1 %	0.01 %	*(32 %)*
URM	50	40	1	10279
	0.5 %	0.4 %	0.01 %	*(21 %)*

Table 11
Usability rating at the national scale from time-based risk analyses considering a 50-years time window. The "Exposure" data refers to the total number of buildings considered and the relative percentage with respect to the entire database (in italic and in bracket).

	Unusable short-time	Unusable long-time	Collapsed	Exposure (no. buildings)
RC	3115	965	70	15323
	20 %	6.3 %	0.5 %	*(32 %)*
URM	1510	1620	55	10279
	15 %	16 %	0.5 %	*(21 %)*

both RC and URM similar percentages (approximately 0.5 %) of collapses are expected. The above comments also apply in the case of 1-year time window.

Finally, Table 12 compares the risk estimate resulting for school and residential buildings. Results refer to the time-based risk with 50-years time window. Results for residential buildings have been obtained from MARS DPC-ReLUIS 2019–2021 project [129]. They constitute an update of the NRA2018 and are currently the most consistent with the assessment conducted for school buildings. In fact, analogous methodological approaches have been adopted to develop fragility curves (Section 3.1), the same conversion metric has been implemented for defining the MARS-model (Section 4.2), and consistent criteria for the attribution of the soil class and seismic hazard have been assumed (i.e. the ones implemented in the IRMA platform, Section 5.1). It is worth noting that Table 12 also summarizes the estimate of losses for school buildings by assuming the same consequences functions of residential buildings (i.e. by adopting the values in brackets of Table 8). This additional simulation is useful for quantifying the impact on the final result caused by the differences previously discussed on these consequence functions. From Tables 8, it clearly emerges that the risk resulting in Table 12 for schools - which is higher than that expected for residential buildings - is mainly ascribable to the difference in the consequence functions rather than in the vulnerability model. In fact, the percentages summarized in Table 12 are overall consistent, with the only notable difference being a slightly higher percentage for schools ascribable to the vulnerability components. This finding aligns with what already emerged from a more detailed comparison of the fragility curves obtained through the empirical and heuristic approaches by UniNA and UniGE-a [66] for school buildings, and those of the NRA2018 [60] for residential buildings. To summarize, this study highlighted that school buildings are more vulnerable than residential ones in the case of slight to moderate damage, though they are substantially comparable for highest DLs. Specifically, the architectural features of school buildings, such as like large windows in infills or large spans between columns (especially in RC school buildings), may take them more susceptible to damage of non-structural components.

6. Conclusions

In Italy, great attention is given to seismic risk studies. A valuable evidence of is the MARS (Seismic Risk MAps) project, funded in 2019–2021 by the Italian Civil Protection Department with the involvement of ReLUIS consortium with EUCENTRE foundation conveying the effort and expertise of several Italian researchers. The project also included a special task dedicated to the seismic risk assessment of school buildings at the national scale.

The present paper outlines the methodological framework of this research, with a particular emphasis on the consensus-based vulnerability model defined and shared by all the eight research units involved in the project.

Table 12
Usability rating at the national scale from time-based risk analyses considering a 50-years time window. Results of school buildings refer to the use of consequence functions consistent with those adopted for residential buildings (i.e. the ones reported in brackets in Tables 8 and 9).

	Unusable short-time	Unusable long-time	Collapsed	Exposure (no. buildings)
RC (residential)	136042	83708	7513	4284611
	3 %	2 %	0.2 %	
URM (residential)	447871	336590	46163	7903087
	6 %	4 %	0.6 %	
RC (school*)	970	613	70	15323
	6 %	4 %	0.5 %	(32 %)
URM (school*)	715	462	56	10279
	7 %	5 %	0.5 %	(21 %)

Based on the inventory of Italian school buildings provided by the Ministry of Education for the MARS research, dating back to 2005, a specific taxonomy was developed and a comprehensive set of archetypes representative of schools building in Italy was selected. Fragility curves has been derived using 10 different models, 5 of them for URM and 5 for RC building types, belonging to heuristic, mechanical, analytical, empirical and hybrid approaches. The paper critically examines the analogies and differences among these methods. The methods used by the research units to derive the fragility curves were already developed in most cases in previous research, although they were applied to different building typed (i.e., residential buildings). This paper presents the results collectively for the first time, facilitating a comprehensive comparison of the whole set of fragility curves obtained in the MARS project. The curves developed stem from approaches that are very different from one another, and in some cases, the resulting differences are not null even within the same methodological approach. Many factors contribute to these differences, and at the current state of research, it is not possible to further reduce some uncertainties in the knowledge. These differences, due to various factors as debated in the paper, highlight the epistemic uncertainty in fragility curve derivation. Typically, current risk analyses rely on a single method, often overlooking the potential bias this introduces.

The paper's key contribution is the creation of the “MARS-Schools model,” which integrates fragility curves into a unified framework based on the six EMS-98 vulnerability classes. This model leverages results from multiple approaches and clarifies the impact of taxonomy attributes. The MARS methodology offers a replicable process for other countries, emphasizing the need for diverse approaches to better understand seismic response variability and account for epistemic uncertainties.

Future research should aim to quantify this uncertainty more precisely and explore ways to minimize differences. The MARS project's approach, which translates fragility curves into vulnerability class percentages, proves effective for comparing different subtypes and communicating outcomes to decision-makers for risk mitigation planning.

Furthermore, the availability of this model enabled to carry out a risk analysis at a national scale. Specifically, the MARS-Schools vulnerability model has been incorporated in the IRMA-School platform, a tool developed by EUCENTRE to perform risk analyses according to the common probabilistic approach. Exposure data comes from the inventory of Italian school buildings set up by the Ministry of Education in 2005, while seismic hazard information is based on the MPS04 hazard map, released by the INGV and the soil amplification map provided by Ref. [125] for the entire Italian territory.

Results from intensity-based risk analyses have been presented in terms of damage distribution for 475-years return period while those from time-based ones for both 1-year and 50-years time windows. The results indicate that the expected damage tends to align with the most hazardous areas, such as certain provinces of the Northeast of Italy and along the Apennines, in particular for URM school buildings. Additionally, time-based analyses over 50-years time window estimate a significant percentage of schools becoming unusable. Specifically, approximatively 26 % of RC buildings and 31 %, of URM buildings would be unusable due to the potential earthquakes expected in the next 50 years. These results further confirm the bit greater risk for URM school buildings compared to RC ones.

Risk results have been compared with those produced in 2018 for residential buildings and they highlight a higher seismic risk for school buildings. This result is ascribable more to the different consequence functions adopted for two asset types than a strong difference in the vulnerability model. It is worth recalling that these consequence functions have been calibrated for the two architectural types (i.e. residential and school buildings) based on real damage data.

Although significant progress was made in the 2019–2021 MARS project, the ongoing 2022–2026 MARS-2 project addresses various challenges. A key development is the incorporation of a newly updated school inventory from 2022, provided by the Italian Ministry of Education, into the risk analyses. This updated database includes more comprehensive data, such as information on maintenance status and retrofitting interventions, which enables a more accurate assessment of school vulnerabilities and associated risks. Additionally, data on the most commonly adopted strengthening techniques is being collected and analyzed. The new registry will also differentiate the functional areas of each school building, distinguishing between those used exclusively for educational purposes and those that host collective spaces or are designated for specific activities, such as canteen, auditoriums, gyms, and/or swimming pools. This will enhance the analysis of structural vulnerability by considering the key needs and vulnerabilities of these large-span environments.

Finally, in order to enrich the available set of fragility curves, further non-linear dynamic analyses involving archetypes not considered in the 2019–2021 project are being performed. Further archetypes belonging to mixed building types or representative of common practice in specific regions are also being selected and analyzed. That will contribute to extend the risk assessment to the overall building stock since up to now it has been limited to RC and URM schools.

CRediT authorship contribution statement

Serena Cattari: Writing – original draft, Visualization, Validation, Supervision, Software, Methodology, Funding acquisition, Data curation, Conceptualization. **Sara Alfano:** Writing – original draft, Visualization, Investigation, Formal analysis, Data curation. **Vincenzo Manfredi:** Writing – original draft, Visualization, Investigation, Formal analysis, Data curation. **Barbara Borzi:** Writing – review & editing, Methodology, Funding acquisition, Conceptualization. **Marta Faravelli:** Writing – review & editing, Visualization, Formal analysis, Data curation. **Antonella Di Meo:** Formal analysis. **Francesca da Porto:** Writing – review & editing, Methodology, Funding acquisition, Conceptualization. **Elisa Saler:** Writing – review & editing, Investigation, Formal analysis. **Andrea Dall'Asta:** Writing – review & editing, Methodology, Funding acquisition, Conceptualization. **Laura Gioiella:** Writing – review & editing, Investigation, Formal analysis. **Marco Di Ludovico:** Writing – review & editing, Methodology, Funding acquisition, Conceptualization. **Ciro Del Vecchio:** Writing – review & editing, Investigation, Formal analysis. **Carlo Del Gaudio:** Writing – review & editing, Investigation, Formal analysis. **Gerardo Verderame:** Writing – review & editing, Methodology, Funding acquisition, Conceptualization. **Natalino Gattesco:** Writing – review & editing, Methodology, Funding acquisition, Conceptualization. **Ingrid Boem:** Writing – review & editing, Investigation, Formal analysis. **Elena Speranza:** Writing – review & editing, Supervision. **Mauro Dolce:** Writing – review & editing, Supervision. **Sergio Lagomarsino:** Writing – review & editing, Supervision, Methodology, Funding acquisition. **Angelo Masi:** Writing – review & editing, Supervision, Methodology, Funding acquisition, Conceptualization.

Declaration of generative AI and AI-assisted technologies in the writing process

During the preparation of this work the authors used ChatGDP to improve the English quality of the paper. After using this tool, the authors reviewed and edited the content as needed and take full responsibility for the content of the publication.

Declaration of competing interest

The authors declare that they have no known competing financial interests or personal relationships that could have appeared to influence the work reported in this paper.

Acknowledgements

This paper has been developed under the financial support of the Italian Department of Civil Protection (IDPC), within the ReLUIS-DPC 2019-21 and 2022-204 Research Project, which is gratefully acknowledged. Further, the Authors would like to acknowledge other researchers who actively participated to Task 4.7, in particular: Sofia Giusto, Giuseppe Nicodemo, Mauro Onida, and Daria Ottonelli. Finally, the Authors would like to thank the EUCENTRE developers who implemented the IRMA platform, especially Mauro Onida and Marco Pagano.

Data availability

Data will be made available on request.

ANNEX I. In plan view of prototype school buildings adoped for deriving the MARS-School model

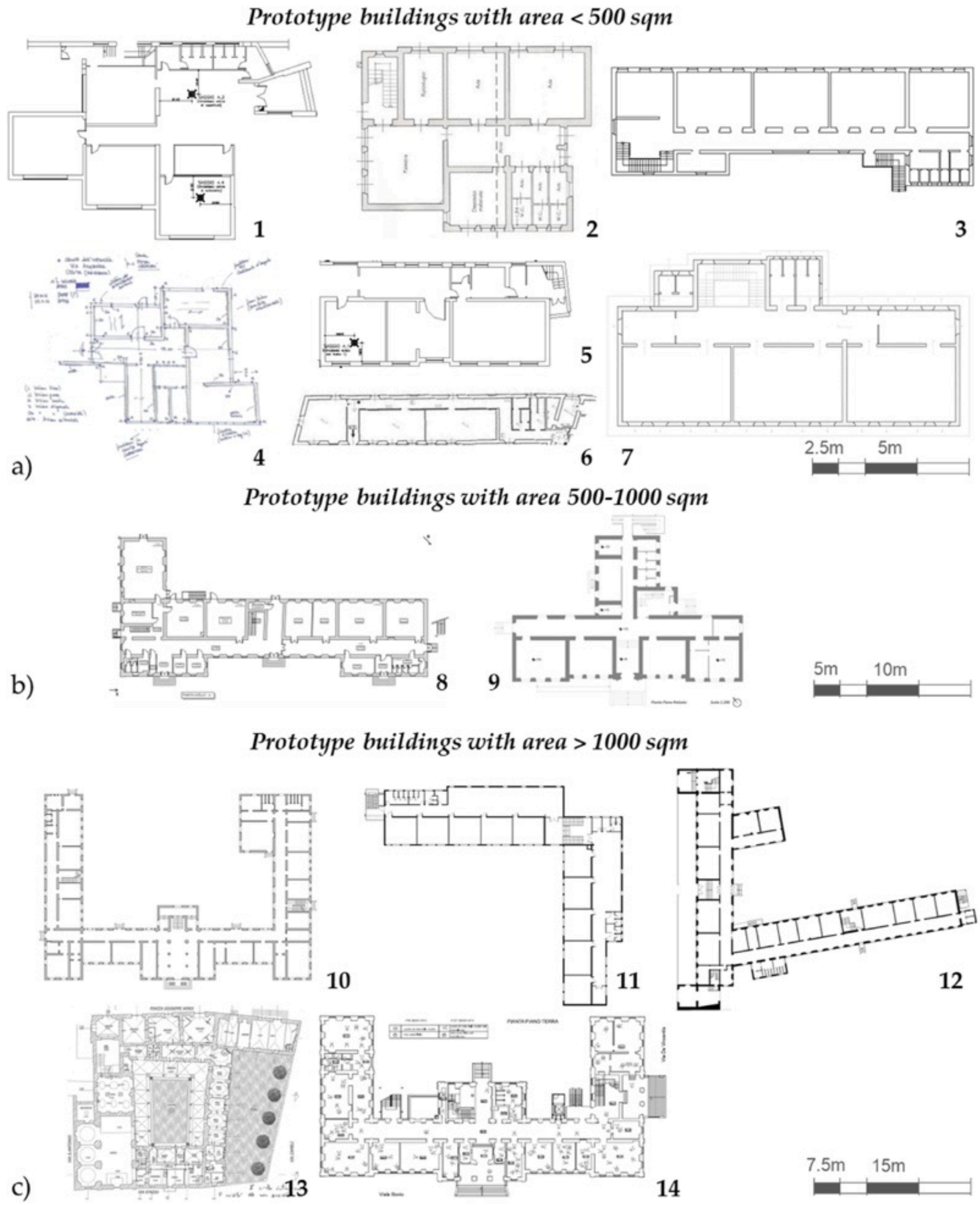

Figure I. Floor plans of URM school building archetypes distinguished by plan area < 500 sqm (a) plan area 500-1,000 sqm (b) and areas > 1,000 sqm (c).

No. archetype	No. of storeys	Age of construction	Type of masonry (for the "as-built" configuration)
1	1	1961-1975	Hollow bricks
2	2/3	1946-1960	Stone ashlar
3	2	1946-1960	Solid bricks
4	1	After 1976	Regular masonry
5	2	1921-1945	Solid bricks

(*continued on next page*)

(*continued*)

No. archetype	No. of storeys	Age of construction	Type of masonry (for the "as-built" configuration)
6	3	Before 1920	Solid bricks
7	2	1921-1945	Simple stone with courses
8	2	1921-1945	Stone ashlar
9	2	1921-1945	Stone ashlar
10	2/3	1921-1945	Simple stone with courses
11	2	1946-1960	Solid bricks
12	2	Before 1920	Solid bricks
13	2	Before 1920	Stone ashlar and solid bricks
14	3	Before 1920	Solid bricks

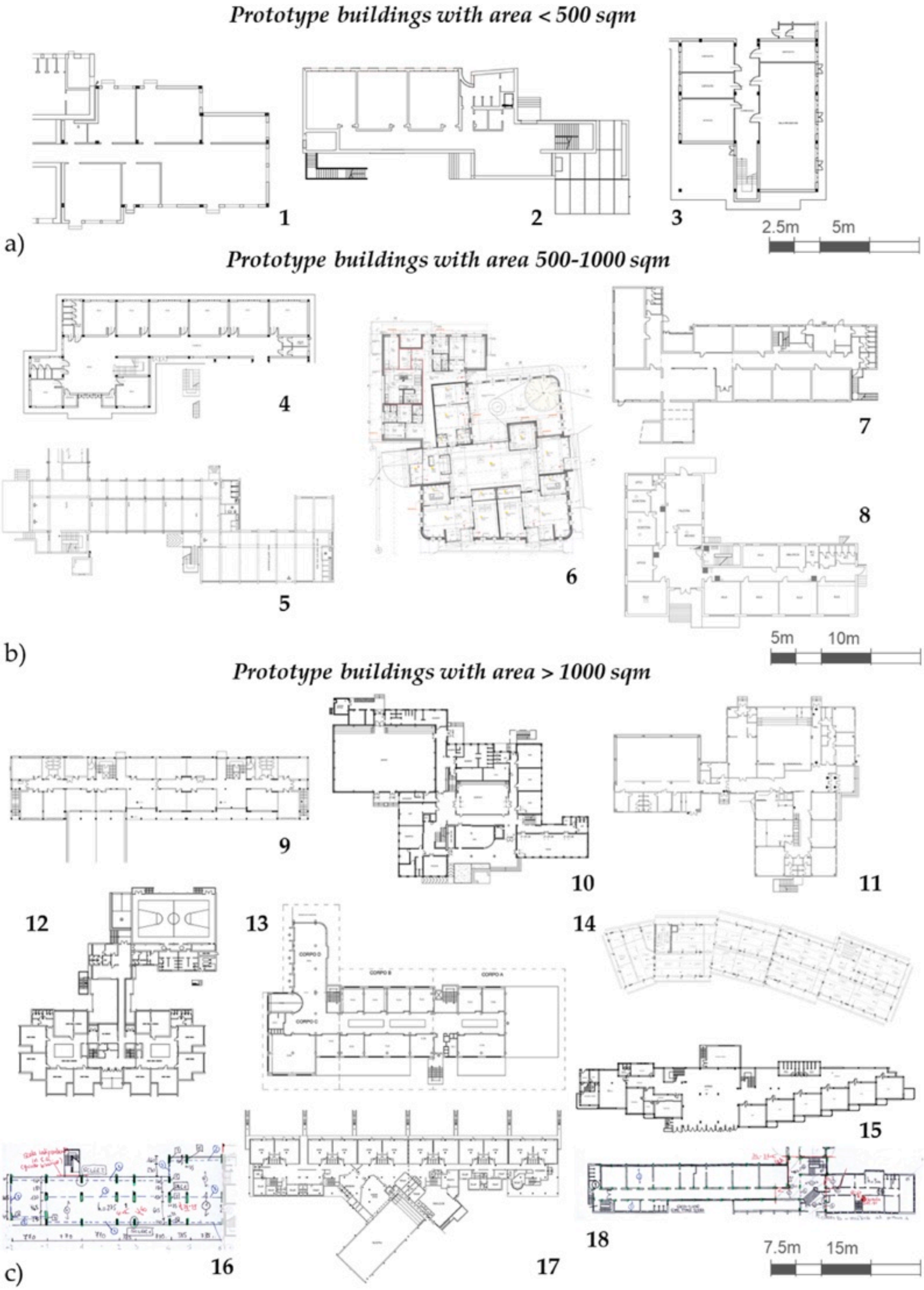

Figure II. Floor plans of RC school building archetypes distinguished by plan area < 500 sqm (a) plan area 500-1,000 sqm (b) and areas > 1,000 sqm (c).

No. archetype	No. of storeys	Age of construction	Design level (for the "as-built" configuration)
1	1	After 1976	Seismic
2	2	After 1976	Seismic
3	2	After 1976	Gravitational
4	2	1961-1975	Gravitational
5	2/3	1961-1975	Gravitational
6	1	After 1976	Seismic
7	2	1961-1975	Gravitational
8	3	1961-1975	Gravitational
9	2	After 1976	Seismic
10	2	After 1976	Gravitational
11	2	1961-1975	Gravitational
12	2	After 1976	Seismic
13	3	After 1976	Seismic
14	3	1961-1975	Gravitational
15	2	1961-1975	Gravitational
16	4	1961-1975	Gravitational
17	3	After 1976	Gravitational
18	4	1961-1975	Gravitational

Appendix A. Supplementary data

Supplementary data to this article can be found online at https://doi.org/10.1016/j.ijdrr.2024.104822.

References

[1] J. Saavedra Chanduvi, M.C. Aedo Inostroza, O.S. Arias Diaz, A. Pushparatnam, M. Gutierrez Bernal, F.H. Rogers, Realizing the future of learning: from learning poverty to learning for everyone, everywhere, Washington, D.C.: World Bank Group. http://documents.worldbank.org/curated/en/250981606928190510/Realizing-the-Future-of-Learning-From-Learning-Poverty-to-Learning-for-Everyone-Everywhere, 2020.

[2] R. Adhikari, D. D'Ayala, R. Fernandez, L. Yamin, A. Nassirpour, A.P. Vatteri, C. Ferreria, F. Ramírez, GLOSI taxonomy: a tool for 'seismic risk assessment' oriented classification of school buildings, Int. J. Disaster Risk Reduc. 87 (2023).

[3] United Stations, Sustainable development goals. The sustainable development goals report, Special edition at. https://unstats.un.org/sdgs, 2023.

[4] The World Bank, Global library of school infrastructure, global program for safer schools (GPSS). https://gpss.worldbank.org/en/glosi.

[5] M. Di Ludovico, A. Digrisolo, C. Moroni, F. Graziotti, V. Manfredi, A. Prota, M. Dolce, G. Manfredi, Remarks on damage and response of school buildings after the Central Italy earthquake sequence, Bull. Earthq. Eng. 17 (2019) 5679–5700.

[6] M. Dolce, E. Speranza, G. De Martino, C. Conte, F. Giordano, The implementation of the Italian National Seismic Prevention Plan: a focus on the seismic upgrading of critical buildings, Int. J. Disaster Risk Reduc. 62 (Issue 9817) (2021) 102391, https://doi.org/10.1016/j.ijdrr.2021.102391.

[7] G.U. 08.05.2003: OPCM n. 3274 del 20.03.2003 – Primi elementi in materia di creteri generali per la classificazione sismica del territorio nazionale e di normative tecniche per le costruzioni in zona sismica, 2003, p. 105 (In italian).

[8] C.E. Ventura, A. Bebamzadeh, M. Fairhurst, M. Turek, G. Taylor, W.D.L. Finn, Performance-based seismic retrofit of school buildings in British Columbia, Canada – an overview, 16th World Conference on Earthquake Engineering, 16WCEE (2017) Santiago Chile.

[9] J. Reyna, Earthquakes and educational infrastructure policy in Mexico, OECD Programme On Educational Building (PEB) and Geohazards International (GHI) (February 2004).

[10] J.E. Rodgers, Why schools are vulnerable to earthquakes. 15th World Conference on Earthquake Engineering, 2012 Lisbon, 24–28 September.

[11] P. Gülkan, Seismic safety of school buildings in Turkey: obstacles impeding the achievable? in: OECD (Ed.), Keeping Schools Safe in Earthquakes, Organization for Economic Cooperation and Development, Paris, 2004, pp. 64–87.

[12] M.K. Naja, H. Baytiyeh, Towards safer public school buildings in Lebanon: an advocacy for seismic retrofitting in-itiative, Int. J. Disaster Risk Reduc. 8 (June 2014) 158–165.

[13] E.A. Peña Figueroa, P. Malisan, S. Grimaz, Implementation of seismic assessment of schools in El Salvador, Int. J. Disaster Risk Reduc. 45 (2020) 101449.

[14] The united Nations office for disaster risk reduction, Sendai Framework for Disaster Risk Reduction (2015) 2030. www.unisdr.org.

[15] The United Nations Office for Disaster Risk Reduction, Worldwide Initiative for Safe Schools, https://www.wcdrr.org/safeschools.html.

[16] The Global Alliance for Disaster Risk Reduction and Resilience in the Education Sector, Comprehensive Safe School Framework, https://gadrrres.net/comprehensive-school-safety-framework/.

[17] Inter-American Development Bank, Learning in twenty-first-century schools, www.iadb.org/education.

[18] S. Grimaz, P. Malisan, UNESCO guidelines for assessing learning Facilities in the context of disaster risk reduction and climate change adaptation. Volume 3 - VISUS Implementation, UNESCO, Paris, 2019, p. 102.

[19] International Finance Corporation, Disaster and Emergency Preparedness: Guidance for Schools, www.ifc.org.

[20] S. Fotopoulou, S. Karafagka, C. Petridis, M. Manakou, E. Riga, K. Pitilakis, Vulnerability assessment of school buildings: generic versus building-specific fragility curves, J. Earthq. Eng. 27 (11) (2023) 2994–3023, https://doi.org/10.1080/13632469.2022.2121791.

[21] A. Karatzetzou, S. Apostolaki, E. Riga, K. Pitilakis, E. Lekkas, Hierarchical policy for seismic intervention of school buildings at urban scale, Structures 48 (2023) 669–680.

[22] S. Karafagka, E. Riga, G. Oikonomou, et al., RiskSchools: a prioritization-based system for the risk assessment of school buildings combining rapid visual screening smartphone app and detailed vulnerability analysis, Bull. Earthq. Eng. (2024), https://doi.org/10.1007/s10518-024-01889-x.

[23] D.N. Grant, J.J. Bommer, R. Pinho, G.M. Calvi, A. Goretti, F. Meroni, A prioritization scheme for seismic intervention in school buildings in Italy, Earthq. Spectra 23 (2) (2007) 291–314.

[24] G.J. O'Reilly, D. Perrone, R. Monteiro, A. Filiatrault, Seismic assessment and loss estimation of existing school buildings in Italy, Eng. Struct. 168 (2018) 142–162.

[25] S. Ruggieri, D. Perrone, M.A. Aiello, A prioritization RVS methodology for the seismic risk assessment of RC school buildings, Int. J. Disaster Risk Reduc. 51 (December 2020) (2020) 101807.

[26] L. Pedone, S. Bianchi, S. Giovinazzi, S. Pampanin, A framework and tool for knowledge-based seismic risk assessment of school buildings: SLaMA-school, Sustainability 14 (2022) 9982, https://doi.org/10.3390/su14169982.

[27] R. Dhungel, R. Guragain, N. Joshi, D. Pradhan, S.P. Acharya, Seismic vulnerability assessment of public-school buildings in Nawalparasi and Lamjung district of

Nepal. 15th World Conference on Earthquake Engineering, 2012 September 24–28, Lisbon (Portugal).
[28] R.K. Adhikari, Parammal, A. Vatteri, D. D'Ayala, Seismic performance assessment of low-rise unreinforced and confined brick masonry school buildings using the applied element method, Buildings 13 (2023) 159, https://doi.org/10.3390/buildings13010159.
[29] R. Fernández, L. Yamin, D. D'Ayala, et al., A simplified component-based methodology for the seismic vulnerability assessment of school buildings using nonlinear static procedures: application to RC school buildings, Bull. Earthq. Eng. 20 (2022) 6555–6585, https://doi.org/10.1007/s10518-022-01445-5.
[30] D. Gautam, R. Adhikari, R. Rupakhety, et al., An empirical method for seismic vulnerability assessment of Nepali school buildings, Bull. Earthq. Eng. 18 (2020) 5965–5982, https://doi.org/10.1007/s10518-020-00922-z.
[31] D. Samadian, M. Ghafory-Ashtiany, H. Naderpour, M. Eghbali, Seismic resilience evaluation based on vulnerability curves for existing and retrofitted typical RC school buildings, Soil Dynam. Earthq. Eng. 127 (2019) 105844.
[32] M. Yekrangnia, A. Bakhshi, M.A. Ghannad, et al., Risk assessment of confined unreinforced masonry buildings based on FEMA P-58 methodology: a case study—school buildings in Tehran, Bull. Earthq. Eng. 19 (2021) 1079–1120, https://doi.org/10.1007/s10518-020-00990-1.
[33] M. Zain, M. Usman, S.H. Farooq, T. Mehmood, Seismic vulnerability assessment of school buildings in seismic zone 4 of Pakistan, Adv. Civ. Eng. (2019) 5808256.
[34] S.M. Alcocer, J.C. Arce, D. Murià-Vila, L.R. Fernández-Sola, D.A. Guardia, Assessment of the seismic safety of school buildings in Mexico: a first look, Earthq. Spectra (2020) 130–153, https://doi.org/10.1177/8755293020926184.
[35] E.A. Opabola, C. Galasso, T. Rossetto, E. Meilianda, Y. Idris, S. Nurdin, Investing in disaster preparedness and effective recovery of school physical infrastructure, Int. J. Disaster Risk Reduc. 90 (2023), https://doi.org/10.1016/j.ijdrr.2023.103623.
[36] R. Gentile, C. Galasso, Y. Idris, I. Rusydy, E. Meilianda, From rapid visual survey to multi-hazard risk prioritisation and numerical fragility of school buildings, Nat. Hazards Earth Syst. Sci. 19 (7) (2019) 1365–1386, https://doi.org/10.5194/nhess-19-1365-2019.
[37] D. D'Ayala, C. Galasso, A. Nassirpour, R. Kumar Adhikari, L. Yamin, R. Fernandez, D. Lo, L. Garciano, A. Oreta, Resilient communities through safer schools, Int. J. Disaster Risk Reduc. 45 (2020), https://doi.org/10.1016/j.ijdrr.2019.101446.
[38] E.A. Opabola, C. Galasso, Informing disaster-risk management policies for education infrastructure using scenario-based recovery analyses, Nat. Commun. 15 (325) (2024), https://doi.org/10.1038/s41467-023-42407-y.
[39] D. Perrone, G.J. O'Reilly, A. Filiatrault, Assessing seismic risk in typical Italian school buildings: from in-situ sur-vey to loss estimation, Int. J. Disaster Risk Reduc. 51 (2020) 101807.
[40] A. Masi, S. Lagomarsino, V. Manfredi, G. Nicodemo, The Italian seismic risk maps: an overview of the methodology and results of MARS project. 3rd Euopean Conference on Earthquake Engineering & Seismology, 2022, pp. 3347–3356 Bucharest, Romania.
[41] M. Dolce, A. Prota, B. Borzi, F. da Porto, S. Lagomarsino, G. Magenes, C. Moroni, A. Penna, M. Polese, E. Speranza, G.M. Verderame, G. Zuccaro, Seismic risk assessment of residential buildings in Italy, Bull. Earthq. Eng. 19 (2021) 2999–3032.
[42] Ministerial Decree 18 December 1975, Norme tecniche aggiornate relative alla edilizia scolastica, ivi compresi gli indici minimi di funzionalità didattica, edilizia ed urbanistica, da osservarsi nella esecuzione di opere di edilizia scolastica, 1975 G.U. 2.2.1976 n. 29 (in Italian).
[43] G.U. 5.2.1996: Ministerial Decree 16 January 1996. Norme tecniche relative ai "Criteri generali per la verifica di sicurezza delle costruzioni e dei carichi e sovraccarichi, 1996, p. 29 (in Italian).
[44] Ministerial Decree 3 October 1978, Criteri generali per la verifica della sicurezza delle costruzioni e dei carichi e sovraccarichi, 1978 G.U. 15 November 1978 n. 319 (in Italian).
[45] L.D. Decanini, L. Liberatore, F. Mollaioli, Strength and stiffness reduction factors for infilled frames with openings, Earthq. Eng. Eng. Vib. 13 (3) (2014) 437–454, https://doi.org/10.1007/s11803-014-0254-9.
[46] Ministerial Decree 5 July 1975, Modificazioni alle istruzioni ministeriali 20 giugno 1896 relativamente all'altezza minima ed ai requisiti igienico-sanitari principali dei locali d'abitazione (1975) G.U. 18 July 1975 n. 190 (in Italian).
[47] G. U. 5 December 1987 n: Ministerial Decree 20 November 1987. Norme tecniche per la progettazione, esecuzione e collaudo degli edifici in muratura e per il loro consolidamento, 1978, p. 285 (in Italian).
[48] Royal Decree n. 2229, Norme per la esecuzione delle opere in conglomerato cementizio semplice od armato, 1939 1939, G.U. 18 April 1940 n.92 (in Italian).
[49] Royal Decree n. 193, 18 April 1909 portante norme tecniche ed igieniche obbligatorie per le riparazioni ricostruzioni e nuove costruzioni degli edifici pubblici e privati nei luoghi colpiti dal terremoto del 28 dicembre 1908 e da altri precedenti elencati nel R.D. 15 aprile 1909 e ne designa i Comuni, 1909 G.U. 22 April 1909 n.95 (in Italian).
[50] Royal Decreee-Law 13 March 1927, n. 431, Norme tecniche ed igieniche di edilizia per le località colpite dai terremoti (1927) G.U. 8 April 1927 n. 82. (in Italian).
[51] Royal Decree-Law 25 March 1935, 640 Nuovo testo delle norme tecniche di edilizia con speciali prescrizioni per le località colpite dai terremoti, 1935 G.U. 22 May 1935 n. 120. (in Italian).
[52] Ministerial Decree 19 July 1984, Norme tecniche relative alle costruzioni sismiche (1984) G.U. 30 July 1984 n. 208 (in Italian).
[53] Ministerial Decree 14 January 2008, Norme Tecniche delle Costruzioni (NTC08), G.U. 4 February 2008 n. 29, Suppl. Ordinario n (2008) 30 (In italian).
[54] Ministerial Decree 17 January 2018, Aggiornamento delle "Norme Tecniche per le costruzioni" (NTC18), 2018 G.U. 20 February 2019 n. 42 (in Italian).
[55] H. Crowley, V. Despotaki, V. Silva, J. Dabbeek, X. Romão, N. Pereira, J.M. Castro, J. Daniell, E. Veliu, H. Bilgin, C. Adam, M. Deyanova, N. Ademović, J. Atalic, E. Riga, A. Karatzetzou, B. Bessason, V. Shendova, A. Tiganescu, D. Toma-Danila, Z. Zugic, S. Akkar, U. Hancilar, Model of seismic design lateral force levels for the existing reinforced concrete European building stock, Bull. Earthq. Eng. 19 (2021) 2839–2865, https://doi.org/10.1007/s10518-021-01083-3.
[56] M. Faravelli, B. Borzi, M. Onida, S. Cattari, S. Alfano, A. Masi, V. Manfredi, S. Lagomarsino, An Italian platform for the seismic risk assessment of school buildings, XIX ANIDIS conference Torino. (2022) 11-15 September 2022. *Procedia Structural Integrity*, 2022, 44, pp. 107–114.
[57] G. Grunthal, European macroseismic scale, in: Chaiers du Centre Européen de Géodynamique et de Séismologie, vol. 15, 1998 Luxembourg.
[58] T. Rossetto, D. D'Ayala, I. Ioannou, M. Abdelghani, Evaluation of existing fragility curves, in: SYNER-G: Typology Definition and Fragility Functions for Physical Elements at Seismic Risk. Geotechnical, Geological and Earthquake Engineering, vol. 27, Springer, Dordrecht, 2014, pp. 47–93.
[59] S. Lagomarsino, S. Giovinazzi, Macroseismic and mechanical models for the vulnerability and damage assessment of current buildings, Bull. Earthq. Eng. 4 (4) (2006) 415–443.
[60] F. da Porto, M. Donà, A. Rosti, M. Rota, S. Lagomarsino, S. Cattari, B. Borzi, M. Onida, D. De Gregorio, F.L. Perelli, C. Del Gaudio, P. Ricci, E. Speranza, Comparative analysis of the fragility curves for Italian residential masonry and RC buildings, Bull. Earthq. Eng. 19 (2021) 3209–3252.
[61] A. Rosti, M. Rota, A. Penna, Empirical fragility curves for Italian URM buildings, Bull. Earthq. Eng. 19 (2021) 3057–3076.
[62] A. Rosti, C. Del Gaudio, M. Rota, P. Ricci, M. Di Ludovico, A. Penna, G.M. Verderame, Empirical fragility curves for Italian residential RC buildings, Bull. Earthq. Eng. (2021) 1–19.
[63] F. Braga, M. Dolce, D. Liberatore, A statistical study on damaged buildings and an ensuing review of the MSK76 scale, in: Proceedings of the Seventh European Conference on Earthquake Engineering, 1982 Athens.
[64] S. Lagomarsino, S. Cattari, D. Ottonelli, The heuristic vulnerability model: fragility curves for masonry buildings, Bull. Earthq. Eng. 19 (2021) 3129–3163.
[65] D. Lallemant, A. Kiremidjian, A beta distribution model for characterizing earthquake damage state distribution, Earthq. Spectra 31 (3) (2015) 1337–1352.
[66] M. Di Ludovico, S. Cattari, G.M. Verderame, C. Del Vecchio, D. Ottonelli, C. Del Gaudio, A. Prota, S. Lagomarsino, Fragility curves of Italian school buildings: derivation from L'Aquila 2009 earthquake damage through observational and heuristic approaches, Bull. Earthq. Eng. 21 (2023) 397–432.
[67] L. Gioiella, M. Morici, A. Dall'Asta, Empirical predictive model for seismic damage and economic losses of Italian school building heritage, Int. J. Disaster Risk Reduc. 91 (2023) 103631, https://doi.org/10.1016/j.ijdrr.2023.103631.
[68] M. Morici, C. Canuti, G. Leoni, A. Dall'Asta, Empirical predictive model for seismic damage of historical churches, Bull. Earthq. Eng. 18 (2020), https://doi.org/10.1007/s10518-020-00903-2.
[69] G. De Martino, M. Di Ludovico, A. Prota, C. Moroni, G. Manfredi, M. Dolce, Estimation of repair costs for RC and masonry residential buildings based on damage data collected by post-earthquake visual inspection, Bull. Earthq. Eng. 15 (2017) 1681–1706, https://doi.org/10.1007/s10518-016-0039-9.
[70] S. Lagomarsino, S. Podestà, Seismic vulnerability of ancient churches: II. Statistical analysis of surveyed data and methods for risk analysis, Earthq. Spectra 20

(3) (2004) 5–412, https://doi.org/10.1193/1.1737736.
[71] V. Silva, N. Horspool, Combining USGS ShakeMaps and the OpenQuake-engine for damage and loss assessment, Earthq. Eng. Struct. Dynam. 48 (6) (2019) 634–652, https://doi.org/10.1002/eqe.3154.
[72] I. Iervolino, A. Rosti, A. Penna, M. Giorgio, Damage-informed ground motion and semi-empirical fragility assessment, Earthq. Eng. Struct. Dynam. 53 (11) (2024) 3514–3526, https://doi.org/10.1002/eqe.4184.
[73] L.C. Pagnini, R.S. Vicente, S. Lagomarsino, H. Varum, A mechanical model for the seismic vulnerability assessment of old masonry buildings, Earthq Struct 2 (1) (2011) 25–42.
[74] S. Lagomarsino, S. Cattari, Fragility function of masonry buildings, in: K. Pitilakis, H. Crowley, A.M. Kaynia (Eds.), SYNER-G: Typology Definition and Fragility Functions for Physical Elements at Seismic Risk: Buildings, Lifelines, Transportation Networks and Critical Facilities, 2014.
[75] S. Cattari, S. Alfano, D. Ottonelli, E. Saler, F. da Porto, Comparative study on two analytical mechanical-based methods for deriving fragility curves targeted to masonry school buildings, 8th ECCOMAS COMPDYN Conference (2021) Athens, Greece, 27-30 June 2021, pp. 3155-3175.
[76] S.A. Freeman, The capacity spectrum method as a tool for seismic design, in: Proc. Of 11th European Conference of Earthquake Engineering, 1998 Paris, France.
[77] N. Gattesco, R. Franceschinis, F. Zorzini, A strategy for the seismic vulnerability assess of heritage architecture. 15th World Conference of Earthquake Engineering 15WCEE, 2012, pp. 24–28 September, Lisbon, Portugal.
[78] M. Dolce, E. Speranza, F. Bocchi, C. Conte, F. Giordano, B. Borzi, M. Faravelli, A. Di Meo, V. Pascale, Observed damage database of past Italian earthquakes: the DaD.O. WebGIS, Boll. Geofis. Teor. Appl. 60 (2) (2019) 141–164, https://doi.org/10.4430/bgta0254.
[79] C. Del Gaudio, P. Ricci, G.M. Verderame, G. Manfredi, Urban-scale seismic fragility assessment of RC buildings subjected to L'Aquila earthquake, Soil Dynam. Earthq. Eng. 96 (2017) 49–63.
[80] C. Del Gaudio, P. Ricci, G.M. Verderame, A class-oriented mechanical approach for seismic damage assessment of RC buildings subjected to the 2009 L'Aquila earthquake, Bull. Earthq. Eng. 16 (2018) 4581–4605.
[81] B. Borzi, R. Pinho, H. Crowley, Simplified pushover-based vulnerability analysis for large-scale assessment of RC buildings, Eng. Struct. 30 (2008) 804–820, https://doi.org/10.1016/j.engstruct.2007.05.021.
[82] G.M. Verderame, M. Polese, C. Mariniello, G. Manfredi, A simulated design procedure for the assessment of seismic capacity of existing reinforced concrete buildings, Adv. Eng. Software 41 (2) (2010) 323–335.
[83] D. Vamvatsikos, C.A. Cornell, Direct estimation of the seismic demand and capacity of oscillators with multi-linear static pushovers through IDA, Earthq. Eng. Struct. Dynam. 35 (9) (2006) 1097–1117.
[84] B. Borzi, M. Faravelli, A. Di Meo, Application of the SP-BELA methodology to RC residential buildings in Italy to produce seismic risk maps for the national risk assessment, Bull. Earthq. Eng. 19 (2021) 3185–3208.
[85] A. Bernardini, R. Gori, C. Modena, A structural model for continuous masonry building systems in historical centres, in: Proceedings of the Structural Conservation of Stone Masonry. International Technical Conference, Athens, vol. 31, 1989, pp. 29–36 X.-3. XI. 1989. Conservation structurelle de la maçonnerie en pierre. Conférence internationale technique. Athènes, 31. X.-3. XI. 1989; Athens, Greece.
[86] A. Bernardini, R. Gori, C. Modena, M.R. Valluzzi, Vulnus 4.0 - Automatic Procedure for the Seismic Vulnerability Analysis of Masonry Buildings, 2009 (in Italian).
[87] A. Bernardini, R. Gori, C. Modena, Application of coupled analytical models adn experientail knowledge to seismic vulnerability analyses of masonry buildings, in: A. Koridze (Ed.), Earthquake Damage Evaluation and Vulnerability Analysis of Building Structures, Omega Scientific: Wallingford, United Kingdom, 1990 1-870199-07-3.
[88] M. Ferrini, A. Melozzi, A. Pagliazzi, S. Scarparolo, Rilevamento Della Vulnerabilità Sismica Degli Edifici in Muratura - Manuale per La Compilazione Della Scheda GNDT/CNR di II Livello, Versione Modificata Regione Toscana (2003) (in Italian).
[89] D. Benedetti, V. Petrini, Sulla Vulnerabilita sismica Di Edifici in Muratura: Un Metodo Di Valutazione. A method for evaluating the seismic vulnerability of masonry buildings, L'industria delle costruzioni 149 (1984) 66–74.
[90] F. McKenna, OpenSees: a framework for earthquake engineering simulation, Comput. Sci. Eng. 13 (4) (2011) 58–66.
[91] V. Manfredi, A. Masi, G. Nicodemo, A. Digrisolo, Seismic fragility curves for the Italian RC residential buildings based on non-linear dynamic analyses, Bull. Earthq. Eng. 21 (2023) 2173–2214, https://doi.org/10.1007/s10518-022-01605-7.
[92] CSI. SAP2000, Integrated finite element analysis and design of structures basic analysis reference manual. Computers and Structures, Inc., Berkeley, 2010.
[93] C.B. Haselton, A.B. Liel, S.C. Taylor-Lange, G.G. Deierlein, Calibration of model to simulate response of reinforced concrete beam-columns to collapse, ACI Struct. J. 113 (6) (2016) 1141–1152.
[94] R.K. Dowell, F. Seible, E.L. Wilson, Pivot Hysteresis model -Dowell, Seible & Wilson, ACI Struct. J. 95 (1998) 607–617.
[95] M. Di Ludovico, G.M. Verderame, A. Prota, G. Manfredi, E. Cosenza, Cyclic behavior of non-conforming full scale RC columns, ASCE Journal of Structural Engineering 140 (5) (2016).
[96] R. Frascadore, M. Di Ludovico, A. Prota, G.M. Verderame, G. Manfredi, M. Dolce, E. Cosenza, Local strengthening of RC structures as a strategy for seismic risk mitigation at regional scale, Earthq. Spectra 31 (2) (2015).
[97] E. Spacone, F.C. Filippidou, F.F. Taucer, Fibre beam-column model for non-linear analysis of Rc frames: Part I. Formulation, Earthq. Eng. Struct. Dynam. 25 (1996) 711–725.
[98] MIDAS Information Technology Co. Midas Gen Available online: www.cspfea.net.
[99] B. Stafford Smith, Methods for predicting the lateral stiffness and Strength of multi-storey infilled frames, Build. Sci. 2 (1967), https://doi.org/10.1016/0007-3628(67)90027-8.
[100] R.J. Mainstone, Supplementary Note on the Stiffnesses and Strengths of Infilled Frames, Building Research Establishment, Building Research Station, 1974.
[101] T.B. Panagiotakos, M.N. Fardis, Seismic response of infilled RC frame structures, in: In Proceedings of the Proceedings of the 11th World Conference on Earthquake Engineering, 1996, pp. 1–8.
[102] N. Gattesco, R. Franceschinis, F. Zorzini, A strategy for the seismic vulnerability assess of heritage architecture. 15th World Conference of Earthquake Engineering 15WCEE, 2012, pp. 24–28 September, Lisbon, Portugal.
[103] E. Saler, V. Follador, P. Carpanese, M. Donà, F. da Porto, Development of mechanics-based fragility curves for the Italian masonry school asset, Earthquake Spectra 40 (3) (2024) 1905–1932. https://doi.org/10.1177/87552930241245720.
[104] C. Del Gaudio, M.T. De Risi, G.M. Verderame, Seismic loss prediction for infilled RC buildings via simplified analytical method, J. Earthq. Eng. 26 (11) (2022) 5477–5510.
[105] E. Saler, P. Carpanese, V. Follador, F. da Porto, Derivation of seismic fragility curves of a gravity-load designed RC school building through NLTHA. 8th ECCOMAS COMPDYN Conference, 2021 Athens, Greece, 27-30 June 2021, pp. 3127-3140.
[106] ReLUIS-DPC Project 2019-2021 - Work Package 4: MARS (MAps of Risk and Scenarios of Seismic Damage) - Task 4.7: Fragility Models and Curves for Schools and Other Strategic or Relevant Buildings. (In Italian) (avaible under request).
[107] F. Jalayer, H. Ebrahimian, A. Miano, G. Manfredi, H. Sezen, Analytical fragility assessment using unscaled ground motion records, Earthq. Eng. Struct. Dynam. 46 (15) (2015) 2639–2663.
[108] V. Manfredi, A. Masi, A.G. Özcebe, R. Paolucci, C. Smerzini, Selection and spectral matching of recorded ground motions for seismic fragility analyses, Bull. Earthq. Eng. 20 (2022) 4961–4987.
[109] S. Cattari, G. Magenes, Benchmarking the software packages to model and assess the seismic response of unreinforced masonry existing buildings through nonlinear static analyses, Bull. Earthq. Eng. 20 (2022) 1901–1936, https://doi.org/10.1007/s10518-021-01078-0.
[110] C. Baggio, A. Bernardini, R. Colozza, L. Corazza, M. Della Bella, G. Di Pasquale, A. Goretti, A. Martinelli, G. Orsini, F. Papa, G. Zuccaro, Field Manual for Post-earthquake Damage and Safety Assessment and Short Term Countermeasures (AeDES), European Commission—Joint Research Centre—Institute for the Protection and Security of the Citizen, EUR. 2007 22868.
[111] M. Di Ludovico, A. Prota, C. Moroni, G. Manfredi, M. Dolce, Reconstruction process of damaged residential buildings outside historical centres after the L'

Aquila earthquake: part I: “light damage” reconstruction, Bull. Earthq. Eng. 15 (2) (2017) 667–692, https://doi.org/10.1007/s10518-016-9877-8.
[112] M. Di Ludovico, A. Prota, C. Moroni, G. Manfredi, M. Dolce, Reconstruction process of damaged residential buildings outside historical centres after the L’ Aquila earthquake: part I—“light damage” reconstruction, Bull. Earthq. Eng. 15 (2017) 667–692, https://doi.org/10.1007/s10518-016-9877-8.
[113] T. Rossetto, D. D’Ayala, I. Ioannou, A. Meslem, Evaluation of existing fragility curves, in: K. Pitilakis, H. Crowley, A. Kaynia (Eds.), SYNER-G: Typology Definition and Fragility Functions for Physical Elements at Seismic Risk. *Geotechnical, Geological and Earthquake Engineering*, vol. 27, Springer, Dordrecht, 2014, https://doi.org/10.1007/978-94-007-7872-6.
[114] A. Masi, S. Lagomarsino, M. Dolce, V. Manfredi, D. Ottonelli, Towards the updated Italian seismic risk assessment: exposure and vulnerability modelling, Bull. Earthq. Eng. 19 (2021) 3253–3286.
[115] S. Lagomarsino, The MARS vulnerability model: a new metrics based on EMS-98 vulnerability classes. 3rd Euopean Conference on Earthquake Engineering & Seismology, 2022, pp. 3327–3336 Bucharest, Romania.
[116] J.R. Murphy, L.J. O’Brien, The correlation of peak ground acceleration amplitude with seismic intensity and other physical parameters, Bull. Seismol. Soc. Am. 67 (1977) 877–915.
[117] E. Faccioli, C. Cauzzi, Macroseismic intensities for seismic scenarios estimated from instrumentally based correlations, in: Proceedings of the First European Conference on Earthquake Engineering and Seismology, Geneva, Switzerland, September 3–8, 2006 CD-ROM.
[118] V. Follarod, P. Carpanese, M. Donà, S. Alfano, S. Cattari, S. Lagomarsino, F. da Porto, Comparison of fragility sets to assess the effectiveness of retrofit interventions on masonry buildings in Italy, Buildings 13 (12) (2023) 2937, https://doi.org/10.3390/buildings13122937.
[119] A. Michelini, L. Faenza, G. Lanzano, V. Lauciani, D. Jozinović, R. Puglia, L. Luzi, The new ShakeMap in Italy: progress and advances in the last 10 yr, Seismol Res. Lett. 91 (1) (2020) 317–333, https://doi.org/10.1785/0220190130.
[120] B. Borzi, M. Onida, M. Faravelli, D. Polli, M. Pagano, D. Quaroni, A. Cantoni, E. Speranza, C. Moroni, IRMA platform for the calculation of damages and risks of Italian residential buildings, Bull. Earthq. Eng. 19 (2021) 3033–3055.
[121] V. Silva, Critical issues in probabilistic earthquake loss assessment, J. Earthq. Eng. 22 (9) (2018) 1683–1709, https://doi.org/10.1080/13632469.2017.1297264.
[122] FEMA P-58-1, Seismic Performance Assessment of Buildings - Volume 1 – Methodology, second ed., 2018.
[123] M. Stucchi, A. Akinci, E. Faccioli, P. Gasperini, L. Malagnini, C. Meletti, V. Montaldo, G. Valensise, Mappa di Pericolosità sismica del territorio Nazionale. http://zonesismiche.mi.ingv.it/documenti/rapporto_conclusivo.pdf, 2004 (in italian).
[124] M. Stucchi, C. Meletti, V. Montaldo, H. Crowley, G.M. Calvi, E. Boschi, Seismic hazard assessment (2003–2009) for the Italian building code, Bull. Seismol. Soc. Am. 101 (4) (2011) 1885–1911.
[125] F. Mori, A. Mendicelli, M. Moscatelli, G. Romagnoli, E. Peronace, G. Naso, A new Vs30 map for Italy based on the seismic microzonation dataset, Eng. Geol. 275 (2020) 105745.
[126] GEM. The OpenQuake-engine User Manual, Global Earthquake Model (GEM) OpenQuake Manual for Engine version 3.16.0 (2022), https://doi.org/10.13117/GEM.OPENQUAKE.MAN.ENGINE.3.16.0.
[127] OPCM n. 3519 del 28.04, Criteri generali per l’individuazione delle zone sismiche e per la formazione e l’aggiornamento degli elenchi delle stesse zone. 2006, G.U. 11.05 (2006) 2006 n. 108.
[128] M. Di Ludovico, G. De Martino, V. Manfredi, A. Masi, A. Prota, L. Sorrentino, M. Zucconi, Loss functions for the risk assessment of residential buildings, Buildings 13 (2023) 2817, https://doi.org/10.3390/buildings13112817.
[129] S. Lagomarsino, A. Masi (a cura di) Report finale: mappe di rischio sismico dell’edilizia residenziale, Report del progetto DPC-ReLUIS 2019-2021 WP4-Mappe di rischio e scenari di danno sismico (MARS) (2021) Italian, available from: ww.reluis.it.